Solar Physics at Low Frequencies

Stephen White

Space Vehicles Directorate
Air Force Research Laboratory

Low frequencies: issues for solar physics

- Always looking to complement solar physics at other wavelengths: energy release, acceleration, etc …
- ”Plasma emission” is a high brightness temperature emission often invoked elsewhere in astrophysics: need to understand it
- Plasma emission as a diagnostic of solar atmosphere, generation of electron beams, electron dynamics in shocks
- Study acceleration in shocks: relevant to astrophysics
- Track CMEs/disturbances through the solar wind, measure speeds to enable forecasting of geomagnetic storm timing (both direct imaging, scintillation, Faraday rotation)

LoFAR Solar Observing

A&A 568, A67 (2014)
DOI: 10.1051/0004-6361/201423936

Astronomy & Astrophysics

LOFAR tied-array imaging of Type III solar radio bursts★

D. E. Morosan[1], P. T. Gallagher[1], P. Zucca[1], R. Fallows[2], E. P. Carley[1], G. Mann[3], M. M. Bisi[4], A. Kerdraon[5], A. A. Konovalenko[6], A. L. MacKinnon[7], H. O. Rucker[8], B. Thidé[9], J. Magdalenić[10], C. Vocks[3], H. Reid[7], J. Anderson[3], A. Asgekar[2,11], I. M. Avruch[12,13], M. J. Bentum[2], G. Bernardi[14], P. Best[15], A. Bonafede[16], J. Bregman[2], F. Breitling[3], J. Broderick[17], M. Brüggen[16], H. R. Butcher[18], B. Ciardi[19], J. E. Conway[20], F. de Gasperin[16], E. de Geus[2], A. Deller[2], S. Duscha[2], J. Eislöffel[21], D. Engels[22], H. Falcke[23,2], C. Ferrari[24], W. Frieswijk[2], M. A. Garrett[2,25], J. Grießmeier[26,27], A. W. Gunst[2], T. E. Hassall[17,28], J. W. T. Hessels[2,29], M. Hoeft[21], J. Hörandel[23], A. Horneffer[30], M. Iacobelli[25], E. Juette[31], A. Karastergiou[32], V. I. Kondratiev[2,33], M. Kramer[30,28], M. Kuniyoshi[30], G. Kuper[2], P. Maat[2], S. Markoff[29], J. P. McKean[2,13], D. D. Mulcahy[30], H. Munk[2], A. Nelles[23], M. J. Norden[2], E. Orru[2], H. Paas[34], M. Pandey-Pommier[35], V. N. Pandey[2], G. Pietka[32], R. Pizzo[2], A. G. Polatidis[2], W. Reich[30], H. Röttgering[25], A. M. M. Scaife[17], D. Schwarz[36], M. Serylak[32], O. Smirnov[37,38], B. W. Stappers[28], A. Stewart[32], M. Tagger[26], Y. Tang[2], C. Tasse[5], S. Thoudam[23], C. Toribio[2], R. Vermeulen[2], R. J. van Weeren[14], O. Wucknitz[39,30], S. Yatawatta[2], and P. Zarka[5]

126 simultaneous beams formed from 24 LOFAR core stations (2 km baselines) with each providing 83 millisec time resolution, 12.5 kHz frequency resolution, 30-90 MHz

LOFAR solar work using 126 tied-array beams

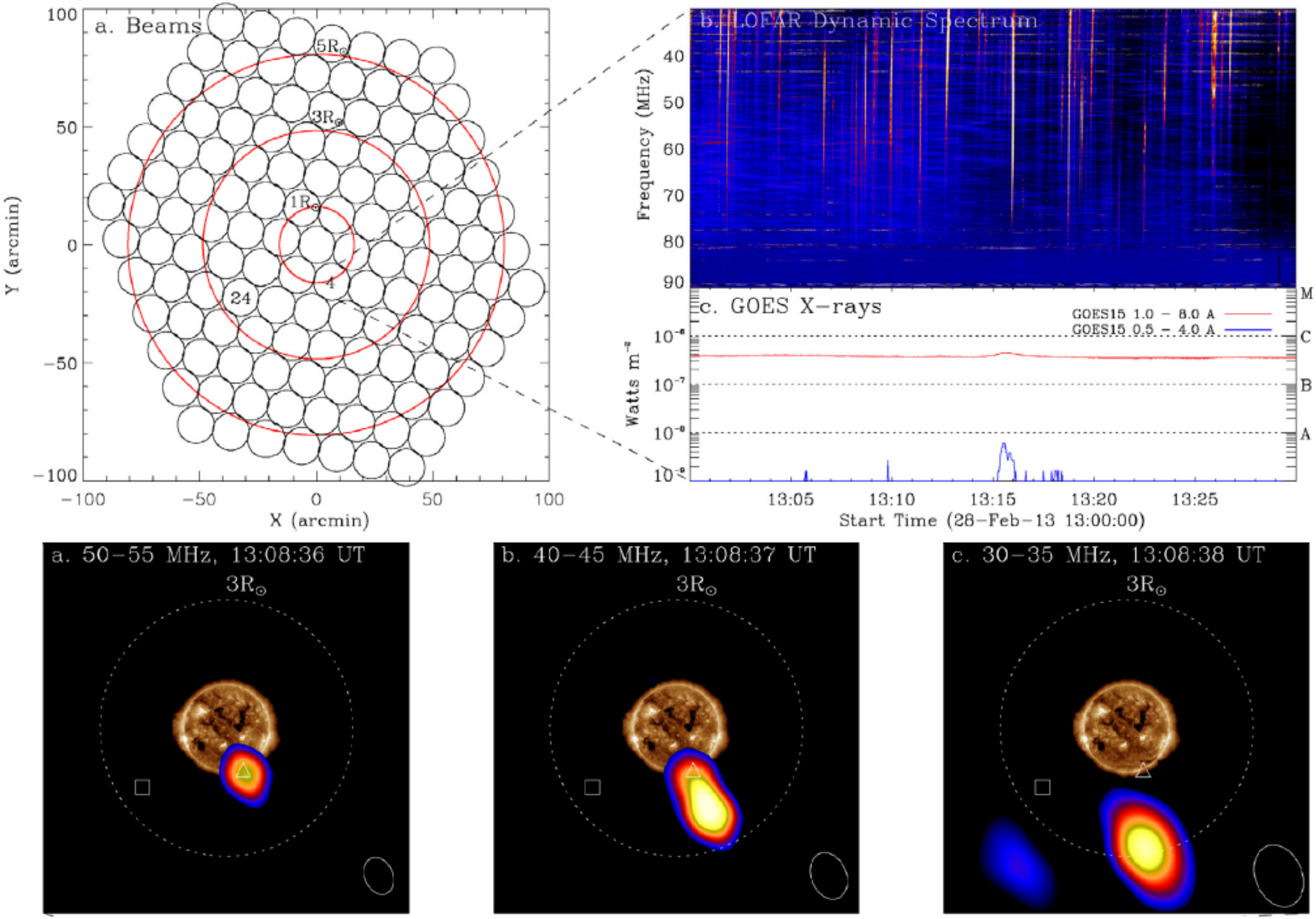

Morosan et al 2014

Type III bursts: 3 frequencies, 2 beam locations

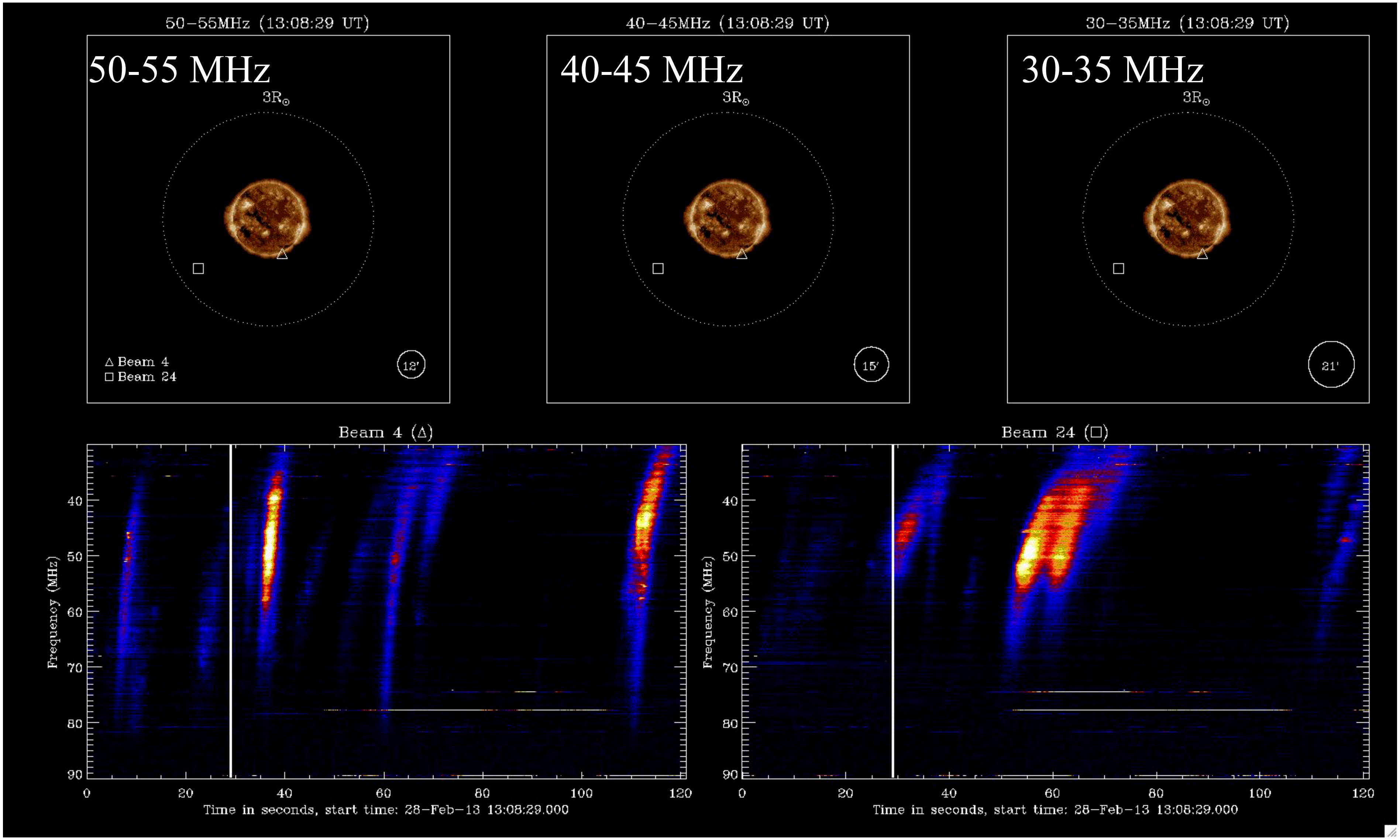

Solar "S bursts" at LOFAR

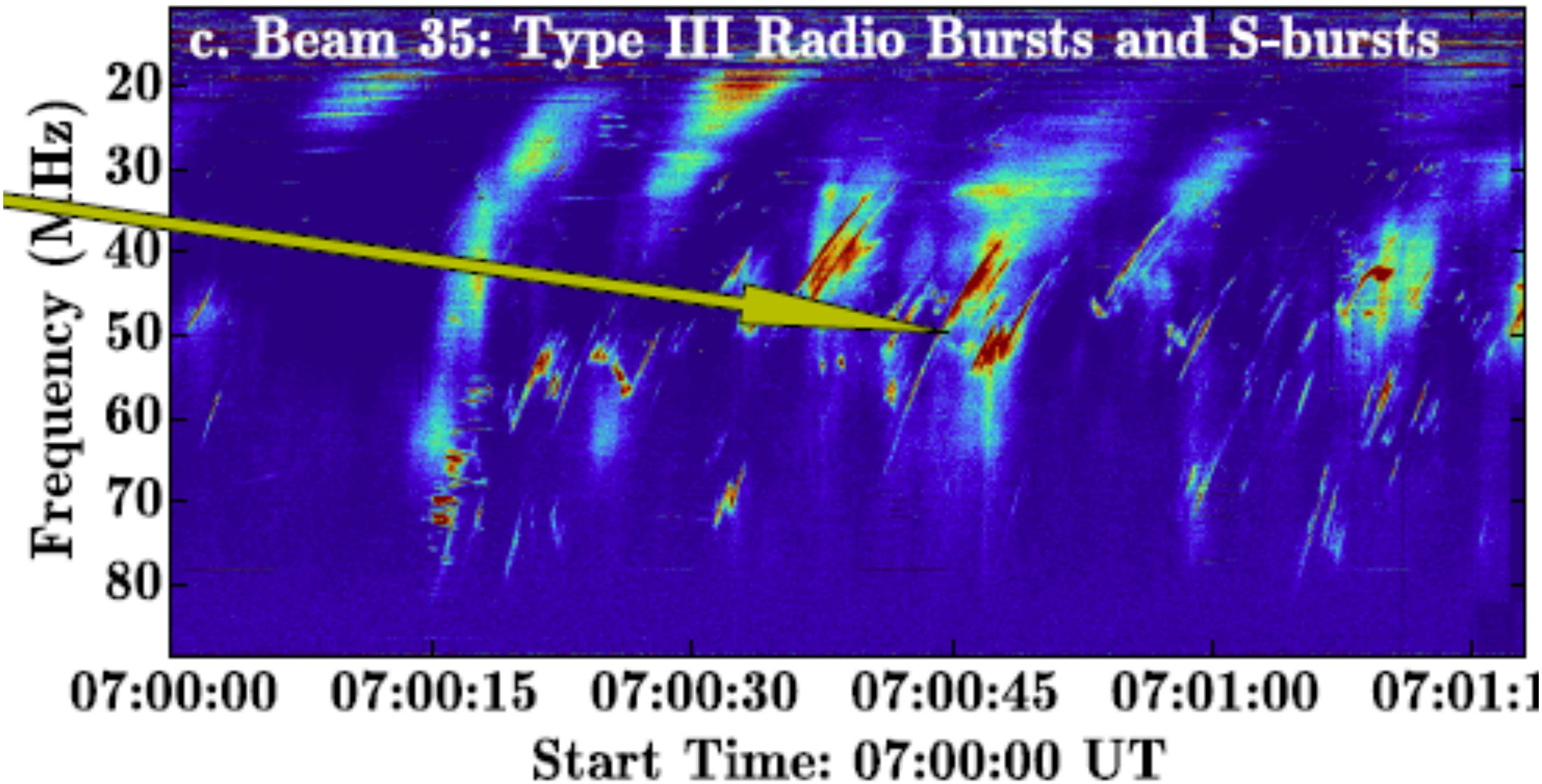

Morosan et al 2015

“S bursts”: Morosan et al 2015

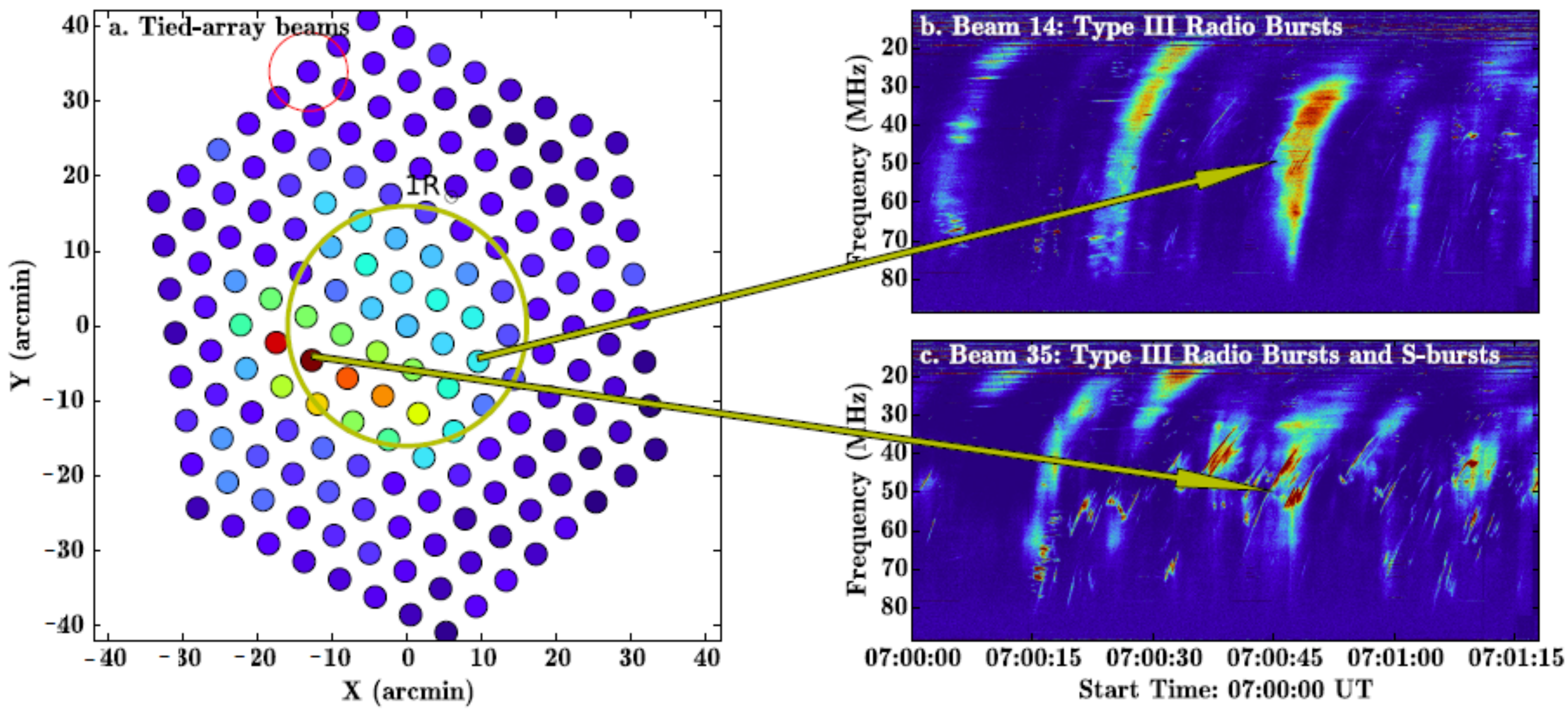

Fig. 1. LOFAR tied-array beam observations of Type III radio bursts and solar S bursts. (a) Map of 170 tied-array beams covering a field-of-view of ~1.3°about the Sun. The full-width half-maximum (FWHM) of the beams at zenith at a frequency of 60 MHz is represented by the red circle and the size of the optical Sun is represented by the yellow circle. (b) Dynamic spectrum recorded for a period of 1.3 minutes corresponding to Beam 14 containing Type III radio bursts. (c) Dynamic spectrum recorded for a period of 1.3 minutes corresponding to Beam 35 containing Type III radio bursts and S bursts. The two arrows indicate the beams that recorded the two dynamic spectra in (b) and (c) pointing at the time and frequency corresponding to the intensity values in (a).

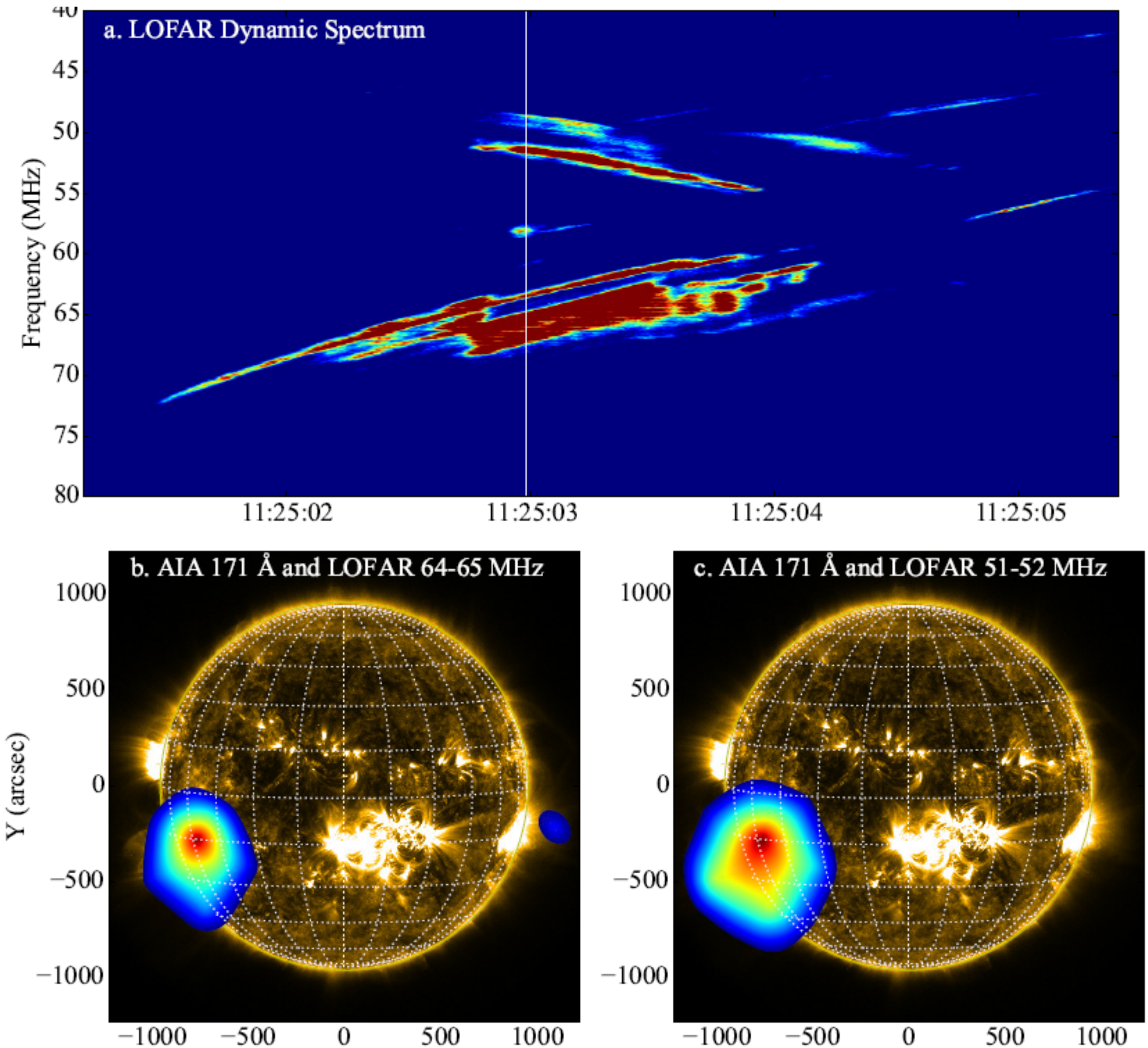
a. LOFAR Dynamic Spectrum
Frequency (MHz)
40
45
50
55
60
65
70
75
80
11:25:02
11:25:03
11:25:04
11:25:05
b. AIA 171 Å and LOFAR 64-65 MHz
c. AIA 171 Å and LOFAR 51-52 MHz
Y (arcsec)
1000
500
0
−500
−1000
−1000
−500
0
500
1000

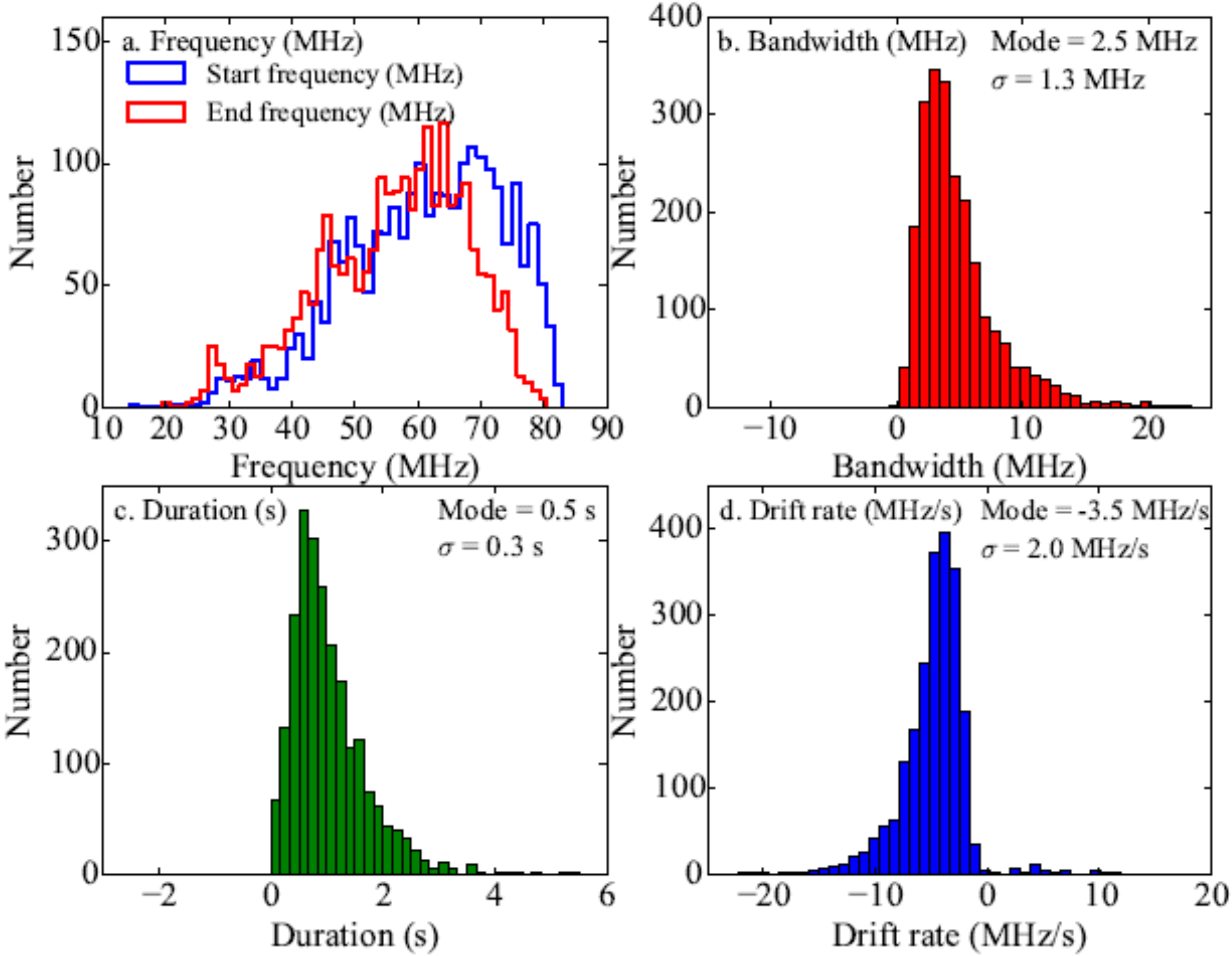
a. Frequency (MHz)
Start frequency (MHz)
End frequency (MHz)
Number
Frequency (MHz)
0
50
100
150
10
20
30
40
50
60
70
80
90
b. Bandwidth (MHz)
Mode = 2.5 MHz
σ = 1.3 MHz
Number
Bandwidth (MHz)
0
100
200
300
400
−10
0
10
20
c. Duration (s)
Mode = 0.5 s
σ = 0.3 s
Number
Duration (s)
0
100
200
300
−2
0
2
4
6
d. Drift rate (MHz/s)
Mode = -3.5 MHz/s
σ = 2.0 MHz/s
Number
Drift rate (MHz/s)
0
100
200
300
400
−20
−10
0
10
20

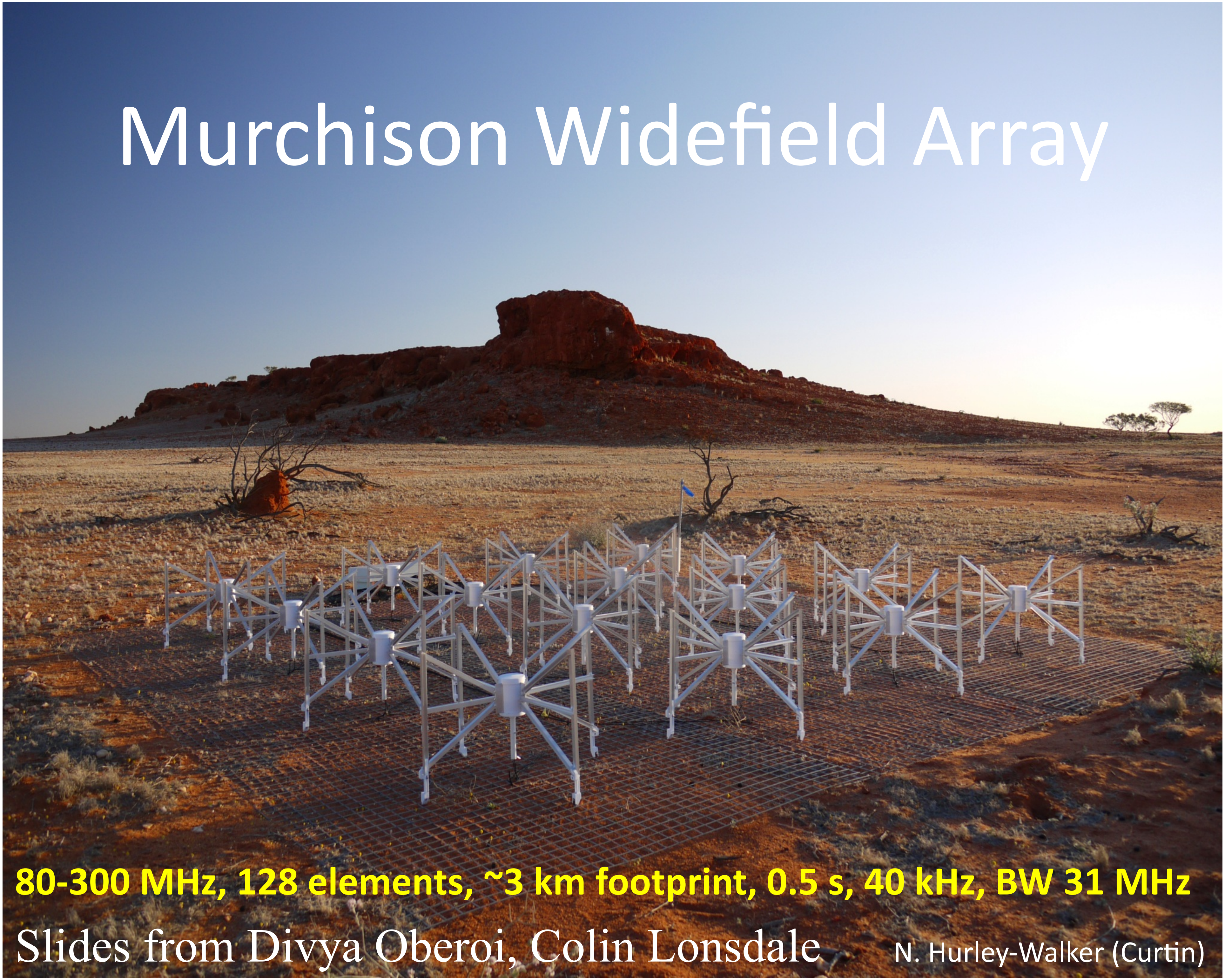
Murchison Widefield Array
80-300 MHz, 128 elements, ~3 km footprint, 0.5 s, 40 kHz, BW 31 MHz
Slides from Divya Oberoi, Colin Lonsdale
N. Hurley-Walker (Curtin)

Quiet vs Active Sun

232.26 MHz

Factor of ~40 between the brightest points on the 2 maps

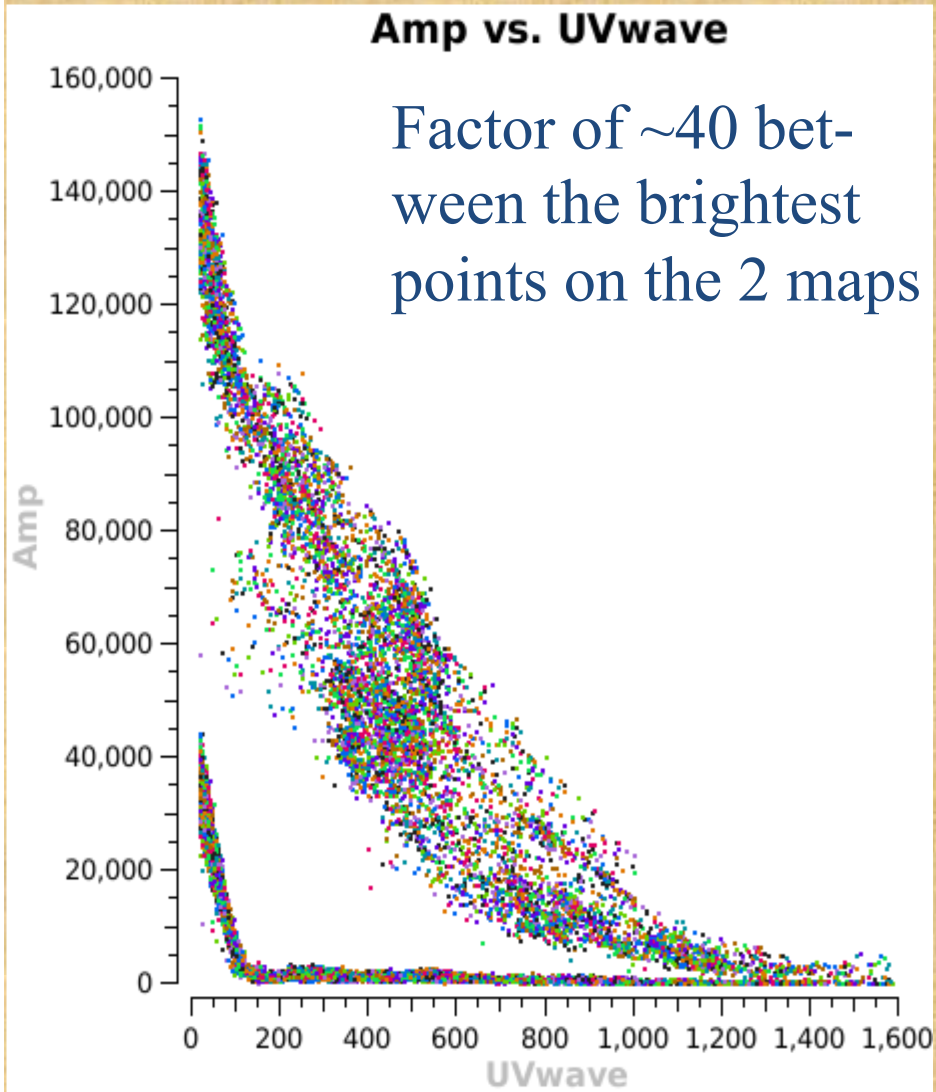

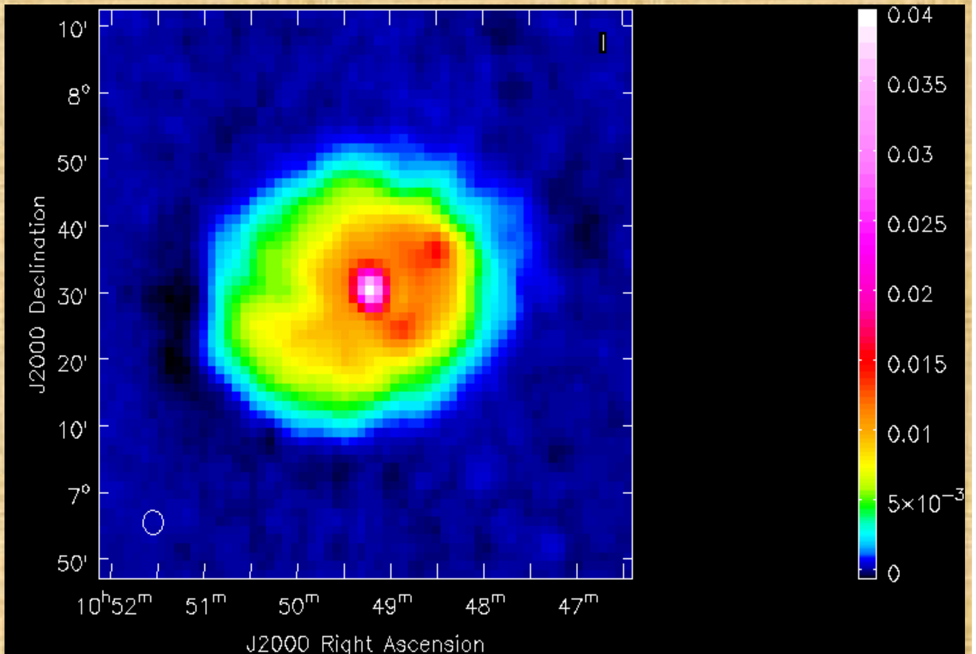

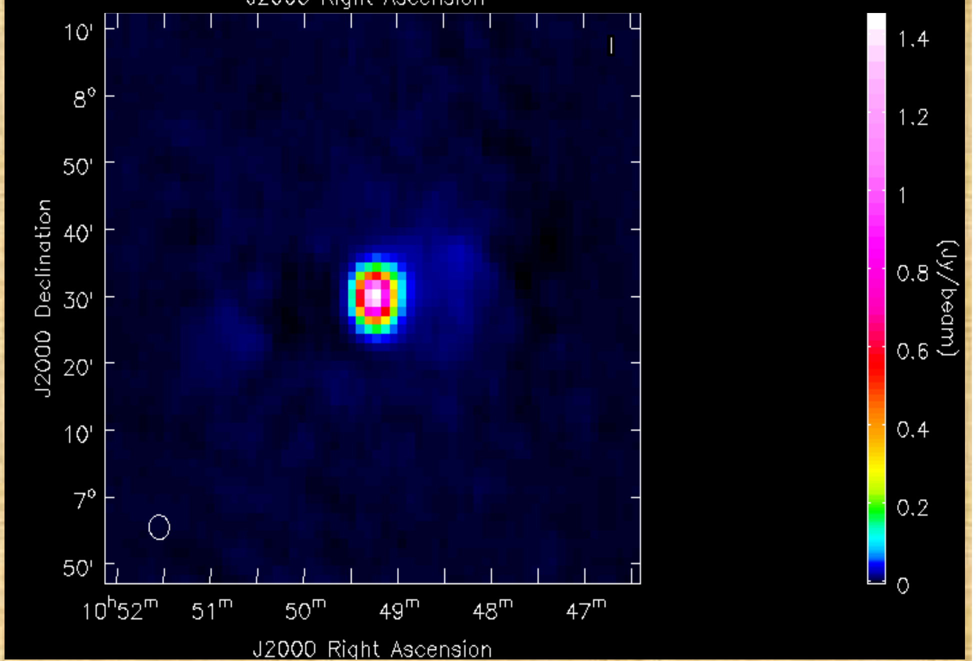

Generalized Van Vleck Correction

- Analog signals have a correlation ρ
- Digital 'CMAC' operation yields κ
- Relationship between ρ and κ is complex …
- Depends on $\boldsymbol{\sigma}_x$, $\boldsymbol{\sigma}_y$, ρ, digitizer levels

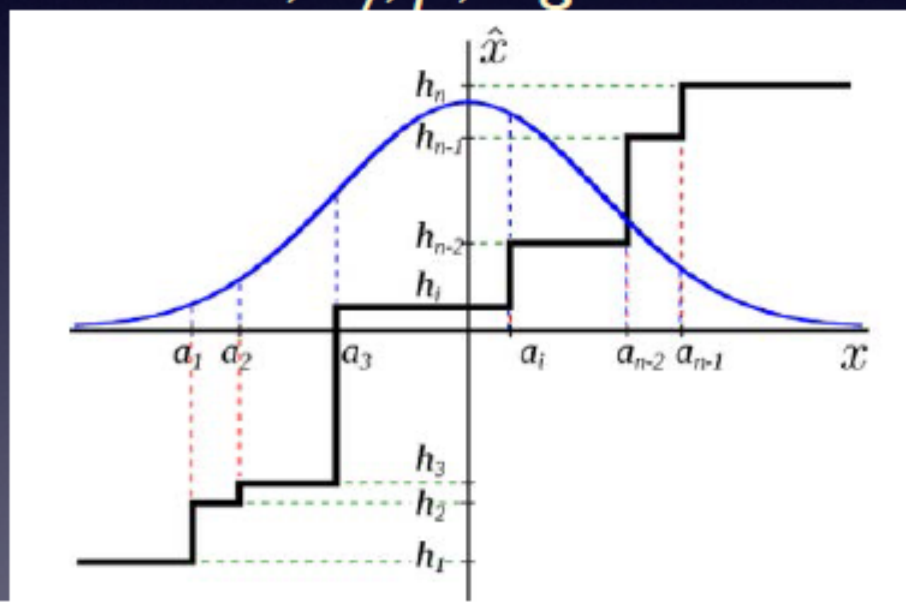

$$\hat{\kappa} = \frac{1}{2\pi} \int_0^{\rho} \frac{1}{\sqrt{1-\zeta^2}} \sum_{i=1}^{n-1} \sum_{k=1}^{n-1} \Delta h_i \Delta h_k \exp\left\{ -\frac{1}{2(1-\zeta^2)} \left[\frac{a_i^2}{\sigma_x^2} + \frac{a_k^2}{\sigma_y^2} - \frac{2\zeta a_i a_k}{\sigma_x \sigma_y} \right] \right\} \mathrm{d}\zeta \tag{20}$$

Haystack: Leo Benkevitch, Colin Lonsdale

The MWA case

- Behaves as a 4-bit 15-level quantizer
- Gaussian behavior verified to high accuracy
- Clips "gracefully" - important for solar
- Large variations in gains from tile to tile
  - Implies $\sigma_x \neq \sigma_y$

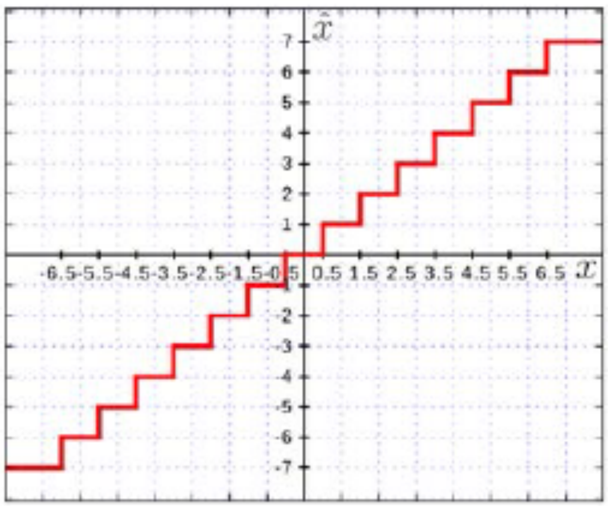

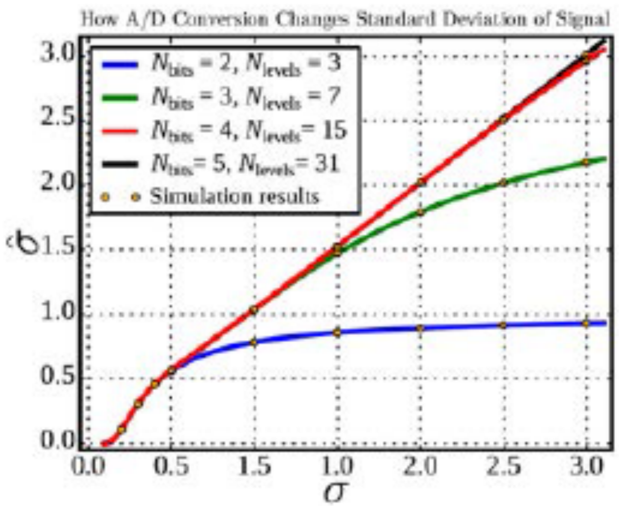

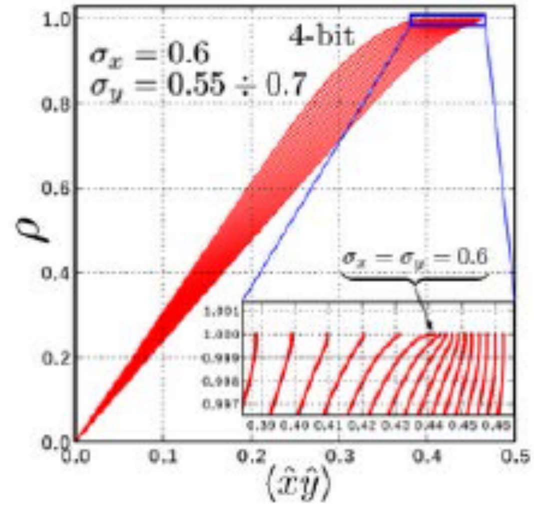

Consequences

- Digital correlator output values are wrong
  - They reflect digital losses
  - The van Vleck losses are **<u>not</u>** a linear function of ρ
  - The errors **<u>cannot</u>** be expressed as station-based scaling factors
  - Errors become significant at high ρ, as in solar work
  - Details in Benkevitch et al. 2015, to be submitted
- Correction software developed for MWA
  - Well-behaved 4-bit digitizer, gaussian signals
  - Unique solutions for a given $\boldsymbol{\sigma}_x$, $\boldsymbol{\sigma}_y$, κ
  - Without correction, errors are many percent

Results to date

- Major improvement using CASA
- Inconsistent results with other packages
- Tracked down errors in correction method
- Definitive testing continues

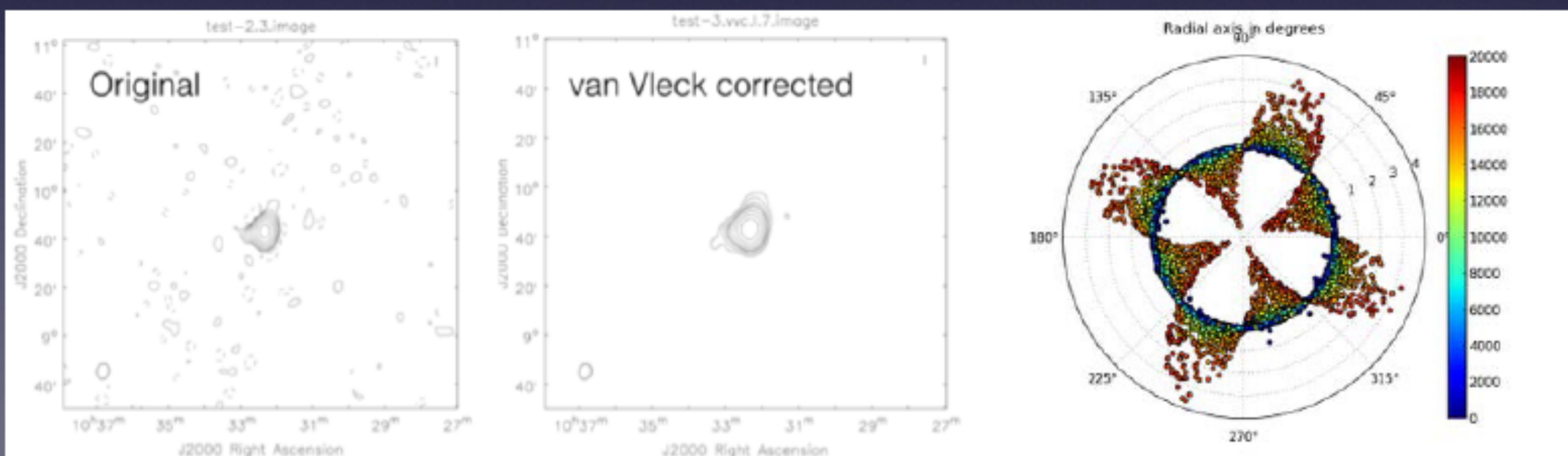

Learmonth Spectrograph

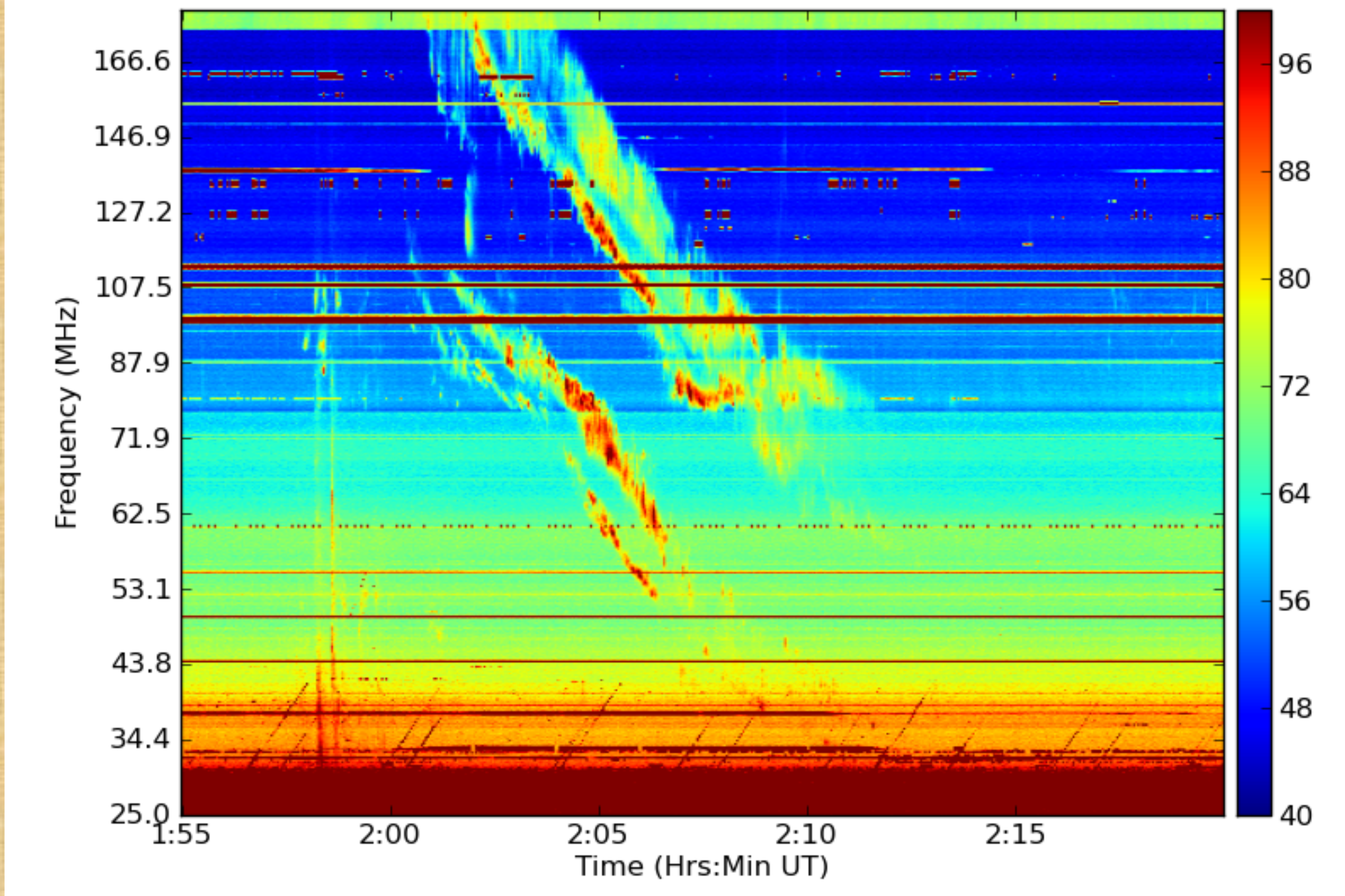

07 September, 2014: Sweep time 3s; Spectral resolution - 125 kHz (25-75 MHz) , 262 kHz (75-180 MHz)

RSTN patrol   Type II burst   2014/09/07

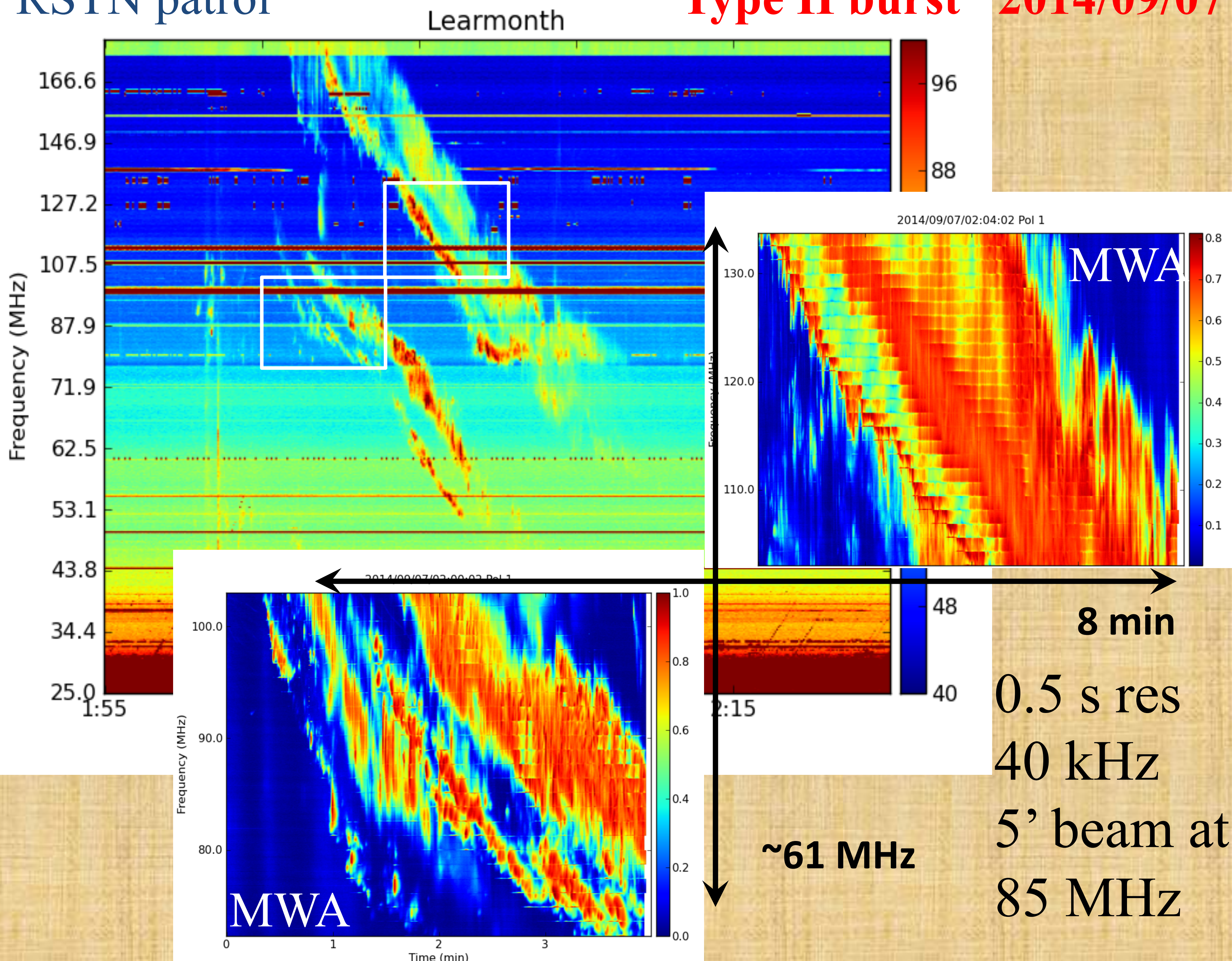

0.5 s res
40 kHz
5' beam at
85 MHz

Make lots of images (Divya Oberoi)

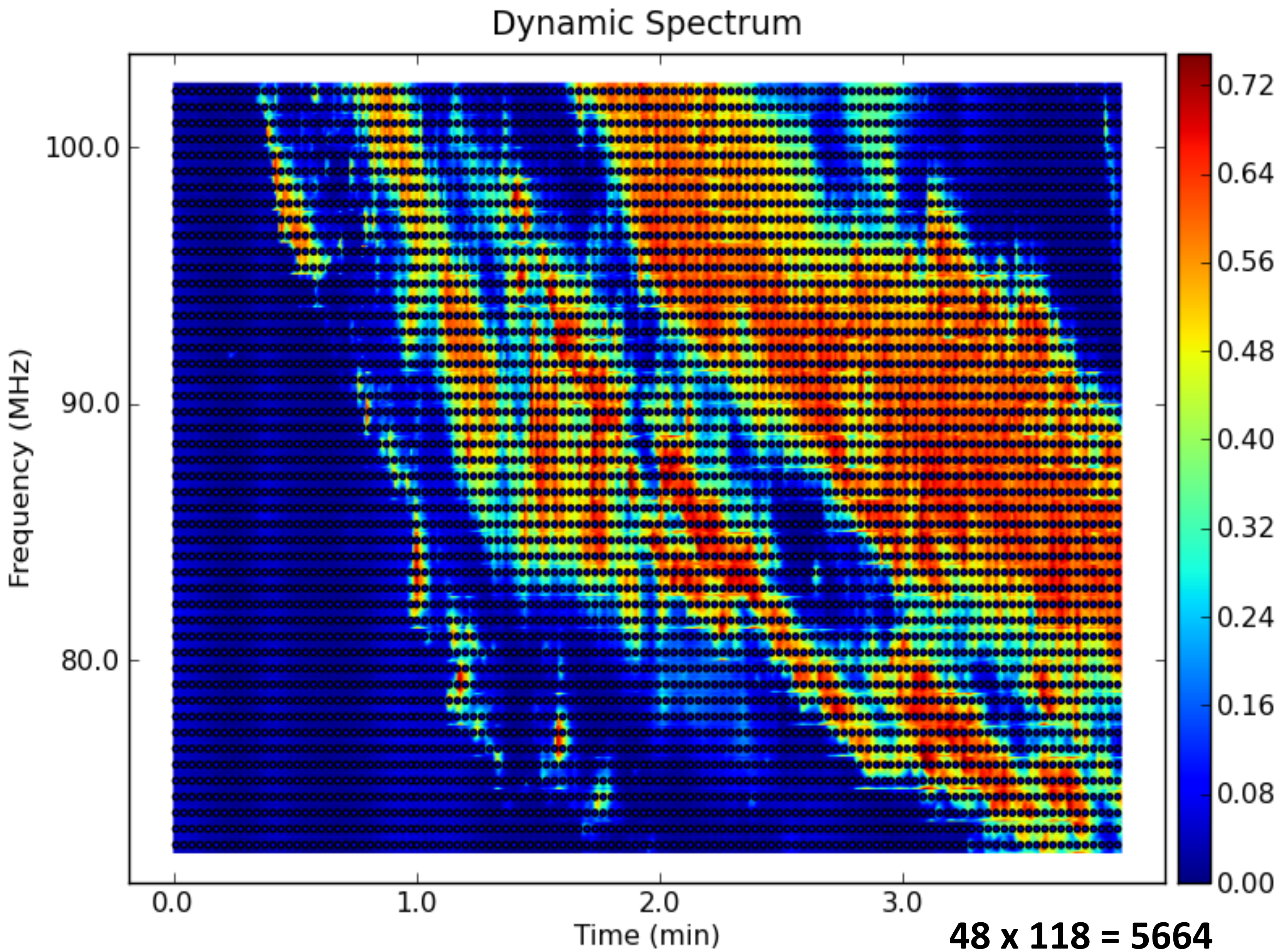

48 x 118 = 5664

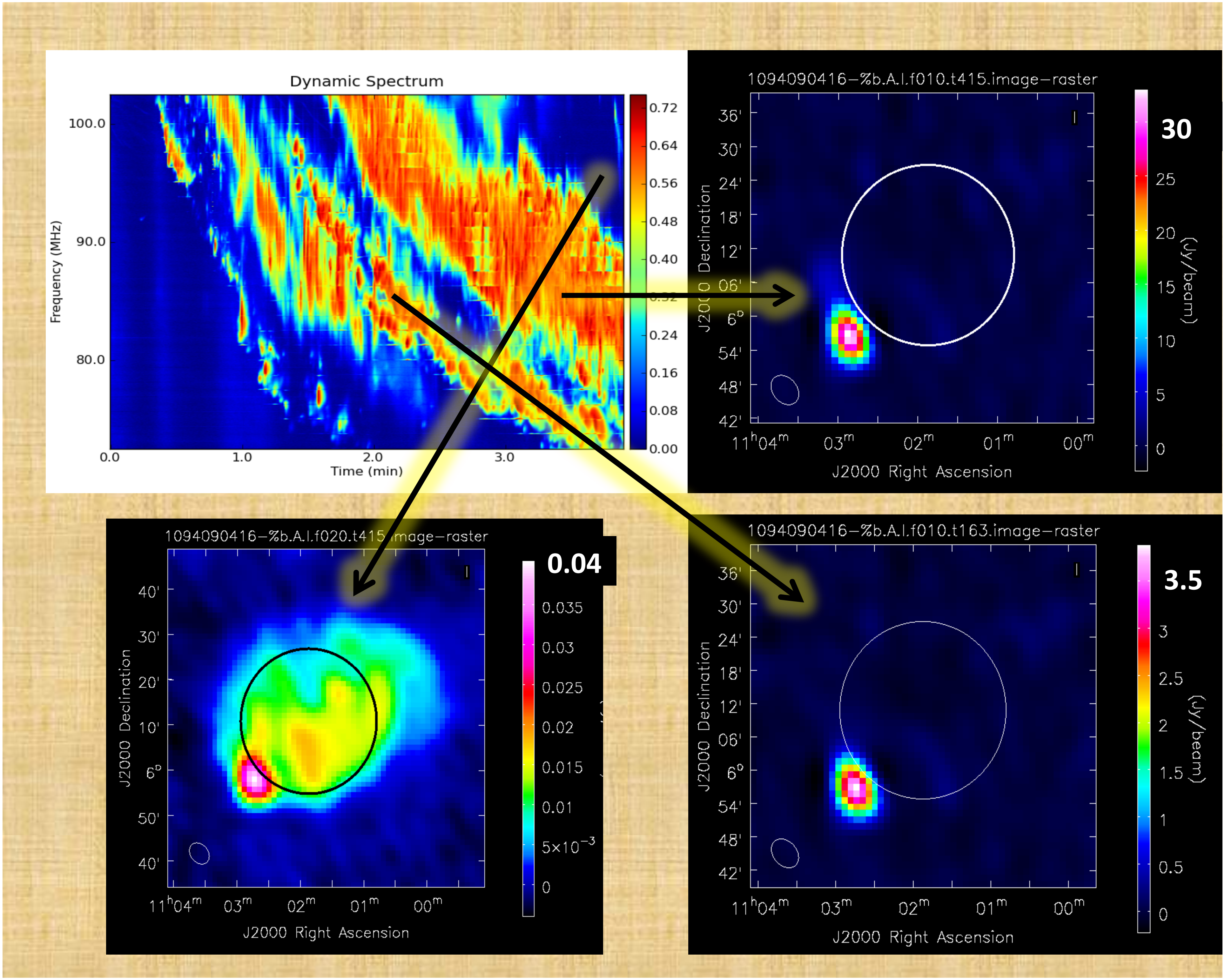
Dynamic Spectrum
Frequency (MHz)
Time (min)
1094090416−%b.A.I.f010.t415.image−raster
30
J2000 Declination
J2000 Right Ascension
(Jy/beam)
1094090416−%b.A.I.f020.t415.image−raster
0.04
1094090416−%b.A.I.f010.t163.image−raster
3.5

Gaussian fit parameters (H)

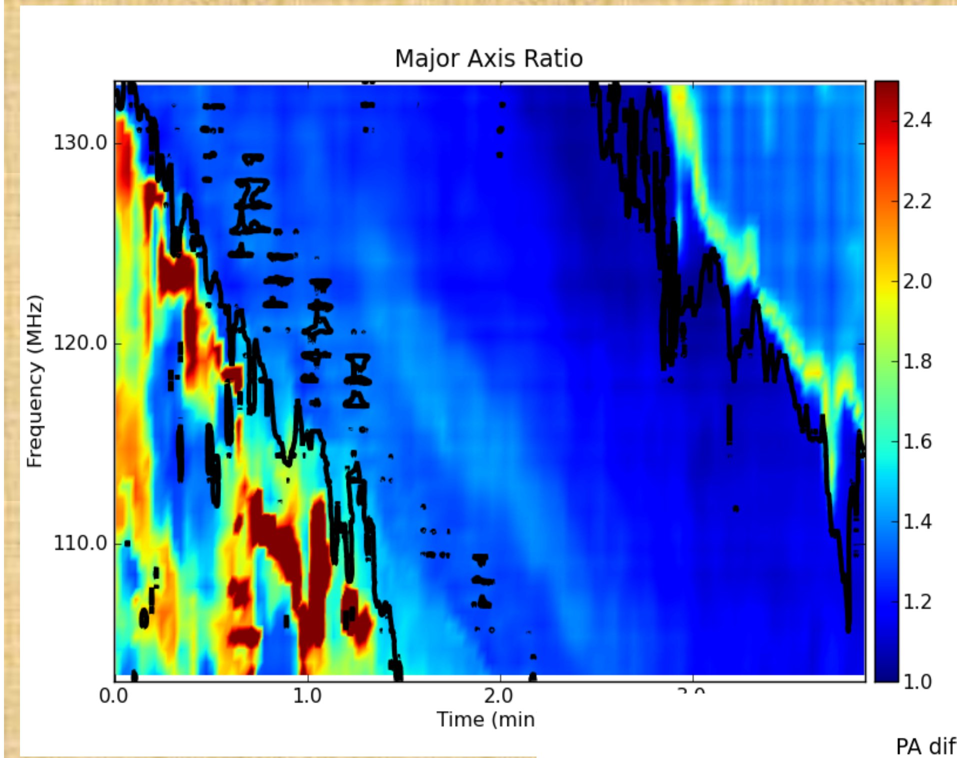

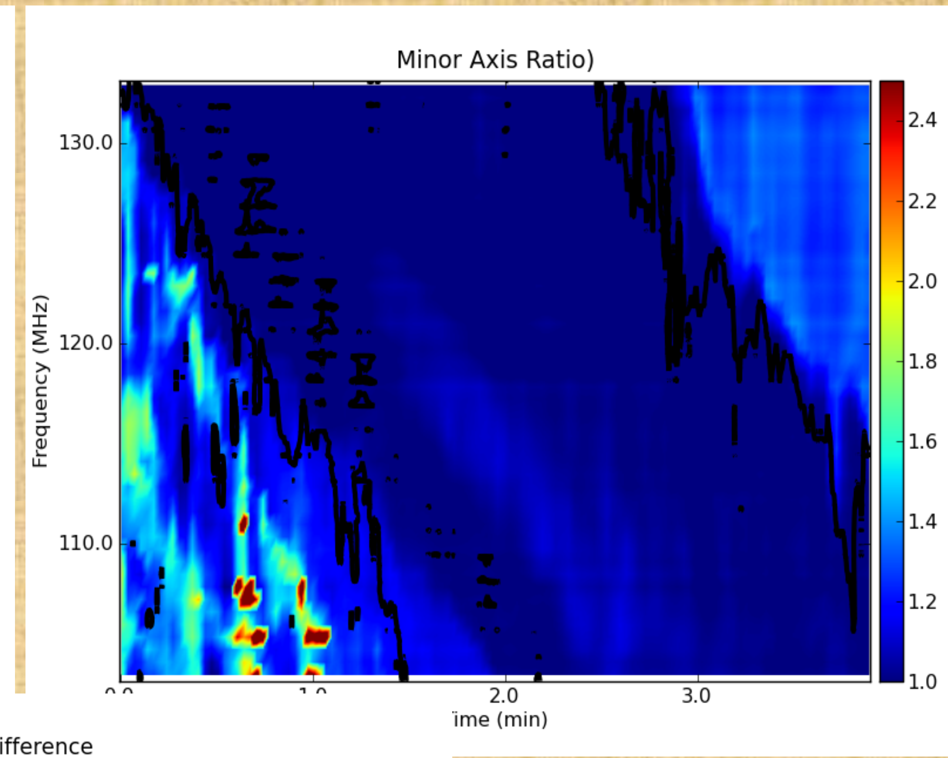

Maj axis: 1.2-1.4 xPSF
Min axis ~1.0-1.2 xPSF
PA diff: -30° to -20°

What is causing the source size to remain nearly constant? Conjecture - strong scattering

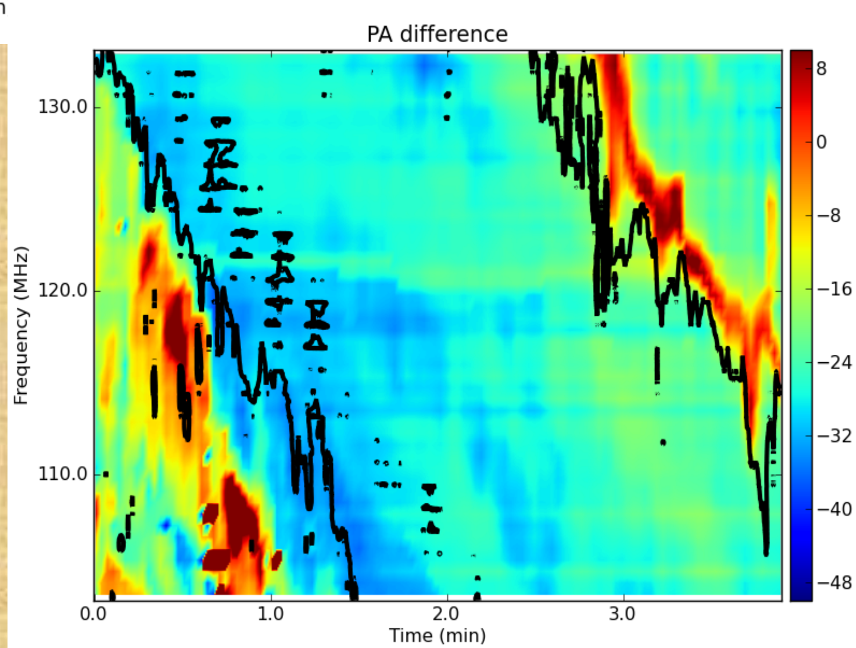

Errors:
Maj axis: <3%
Min axis: <4%
PA diff: <4°

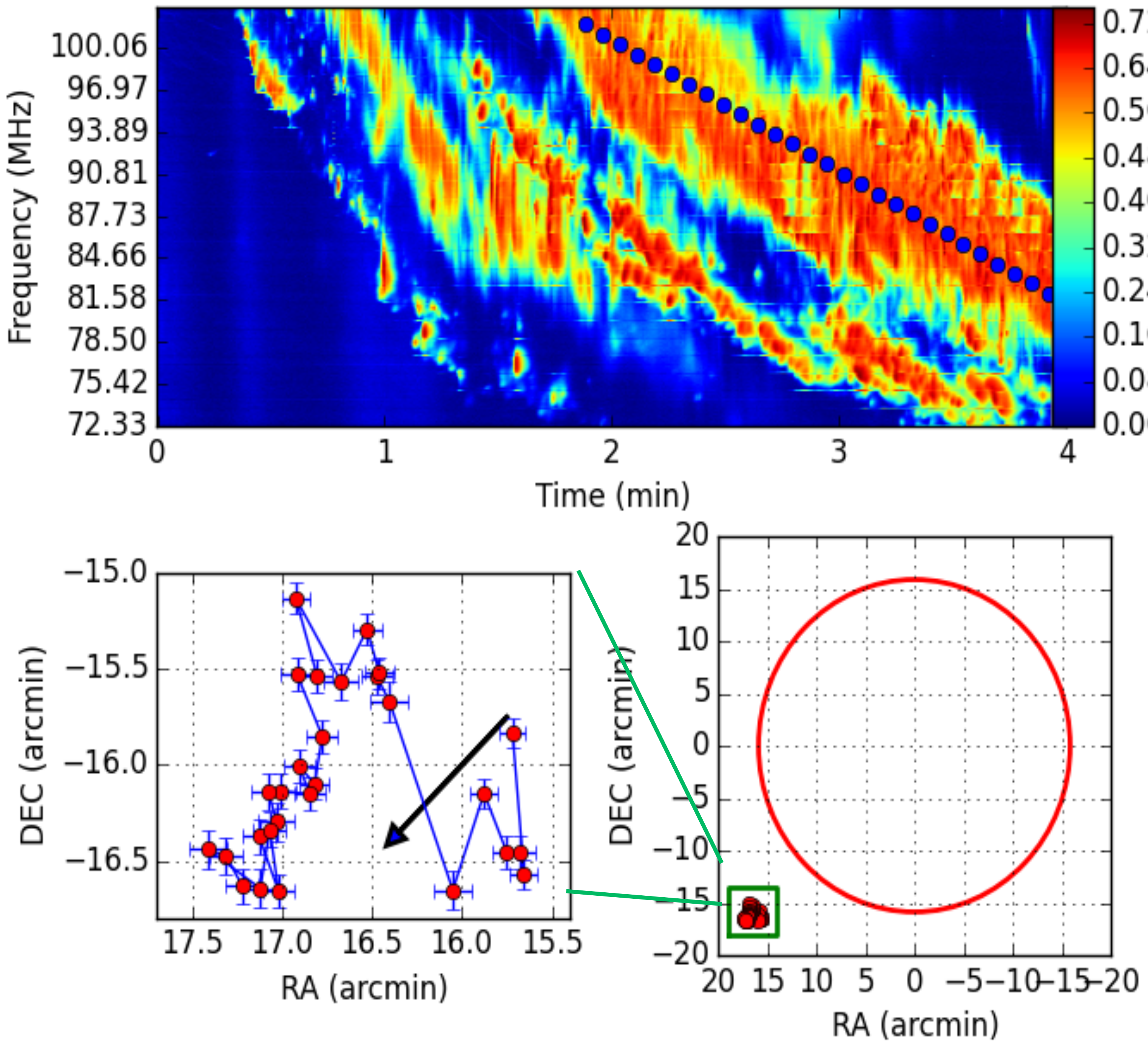

Frequency (MHz)
100.06
96.97
93.89
90.81
87.73
84.66
81.58
78.50
75.42
72.33
0.72
0.64
0.56
0.48
0.40
0.32
0.24
0.16
0.08
0.00
0
1
2
3
4
Time (min)
DEC (arcmin)
−15.0
−15.5
−16.0
−16.5
17.5
17.0
16.5
16.0
15.5
RA (arcmin)
20
15
10
5
0
−5
−10
−15
−20
RA (arcmin)

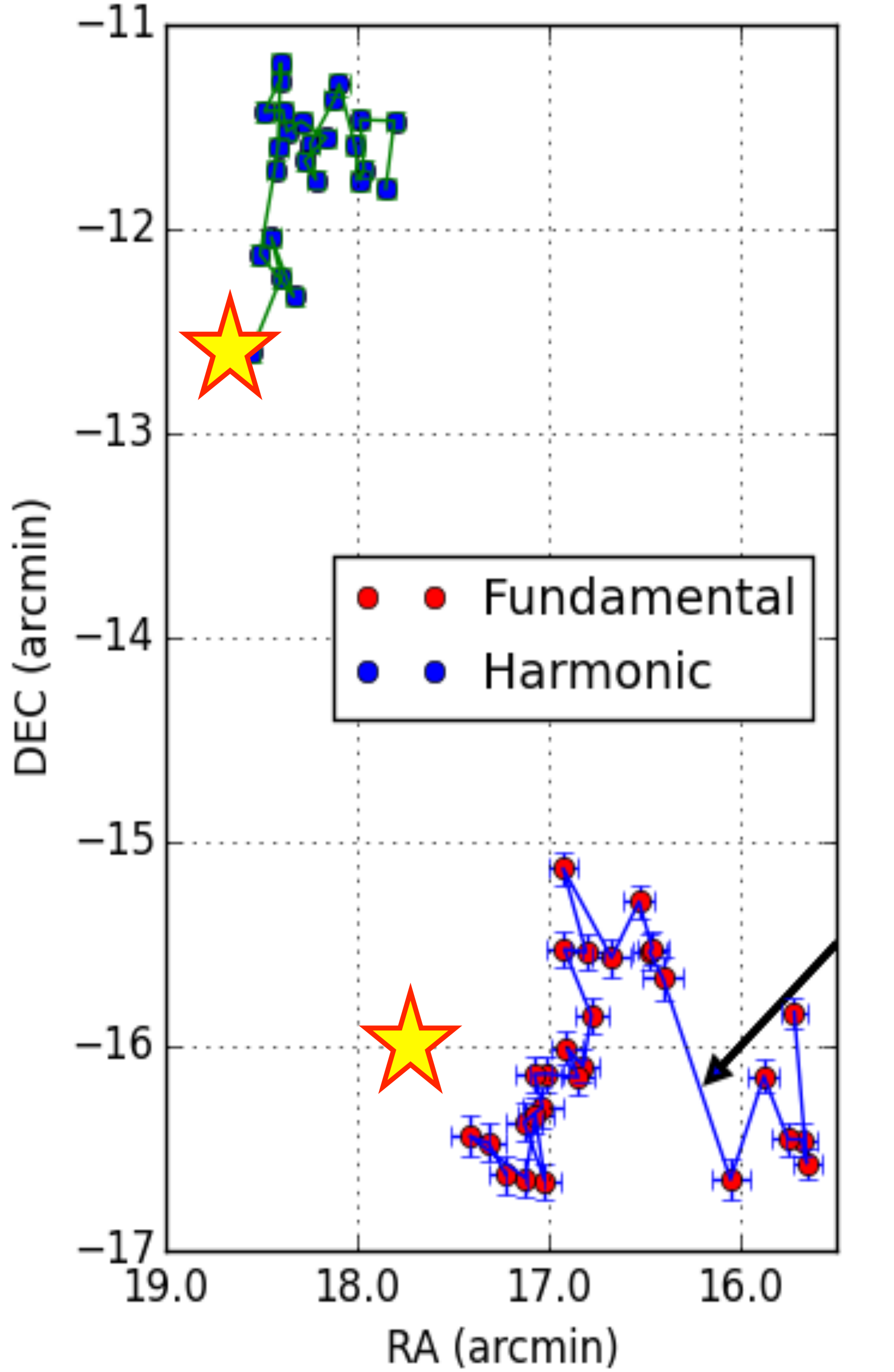

Location of type II source

- Fundamental and Harmonic emission do not appear to be coincident
- Height R_{Sun}:
  1.47 (F), 1.36 (H)

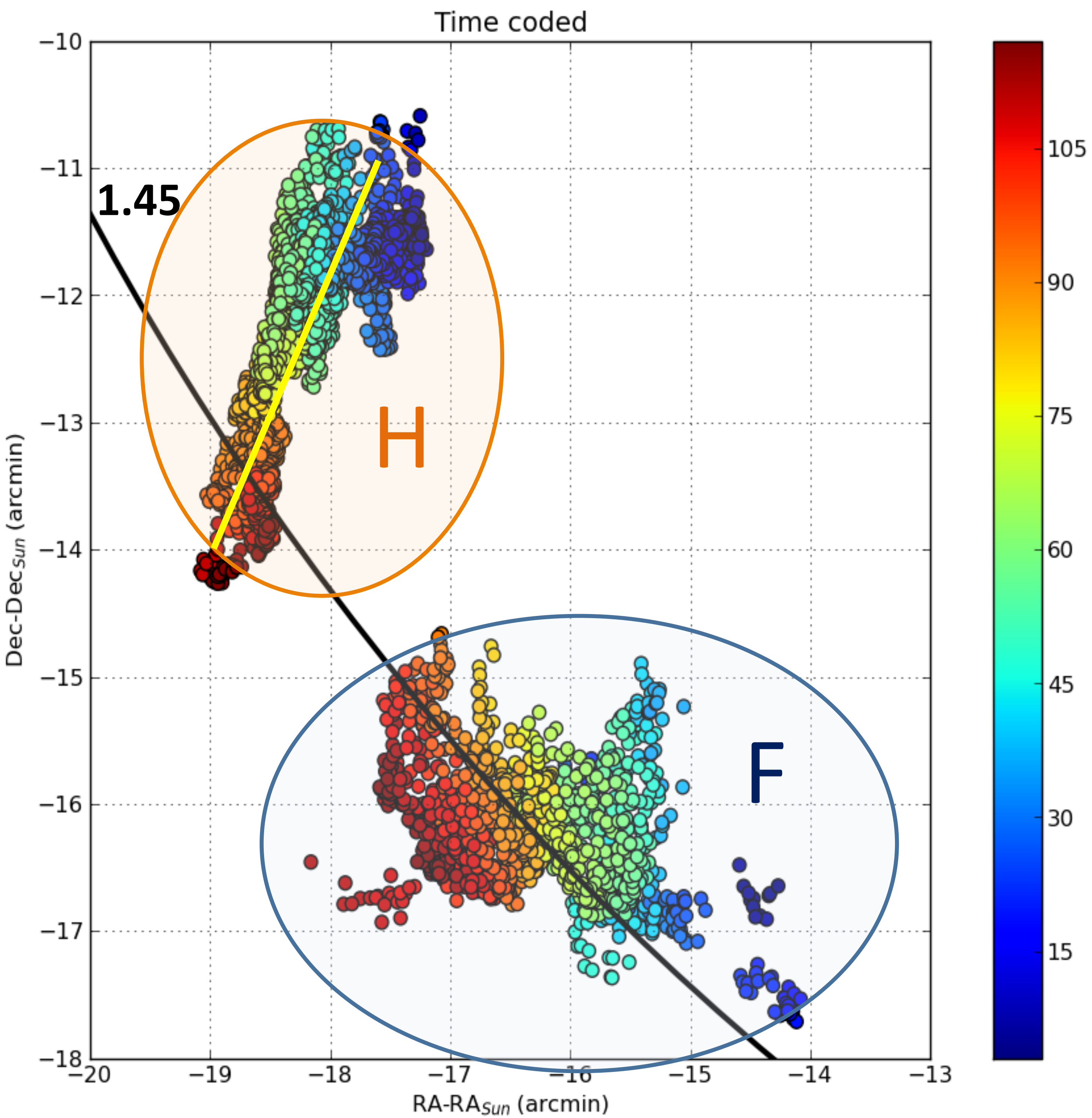

Motion in time

4' @ 1 AU
over 4 min
⇒ 725 km s^{-1}

10-88 MHz usable, Galactic noise-dominated (>4:1) 24-87 MHz
4 independent beams x 2 pol. x 2 tunings each ~16 MHz bandwidth

Beam SEFD ~[6,30] kJy for $Z=[0^{\circ},65^{\circ}]$,
  Also depends on sidereal time, (RA,Dec) of pointing, frequency
  ~ 8 Jy (5σ) for 1 s, 16 MHz, Zenith
Main lobe FWHM < $(4.3^{\circ})((74\ \mathrm{Mhz})/\nu)^{1.5}$ for $Z<45^{\circ}$
Sidelobe levels are high; ~ 10 dB at maxima without much rolloff

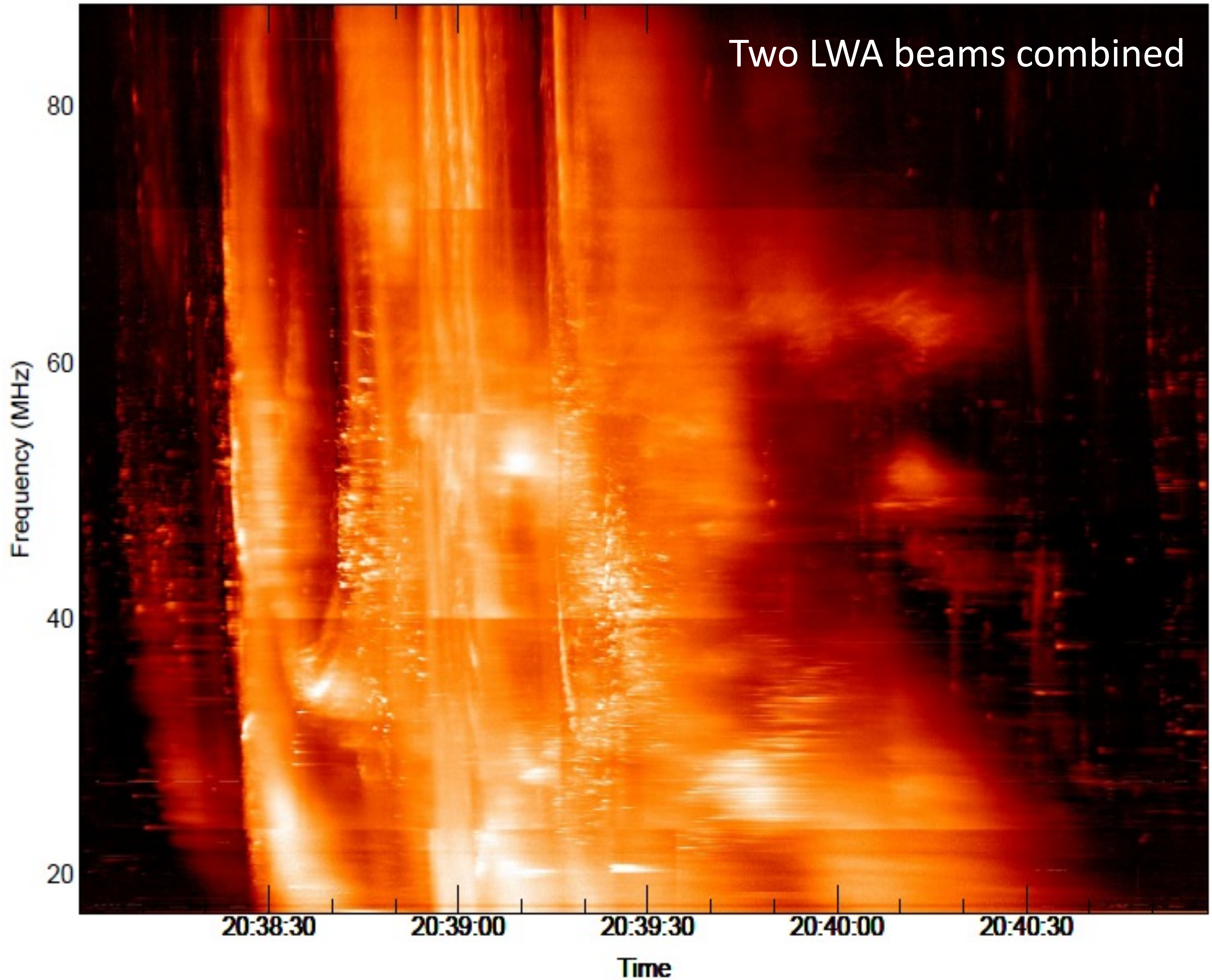

Two LWA beams combined
80
60
40
20
Frequency (MHz)
20:38:30
20:39:00
20:39:30
20:40:00
20:40:30
Time

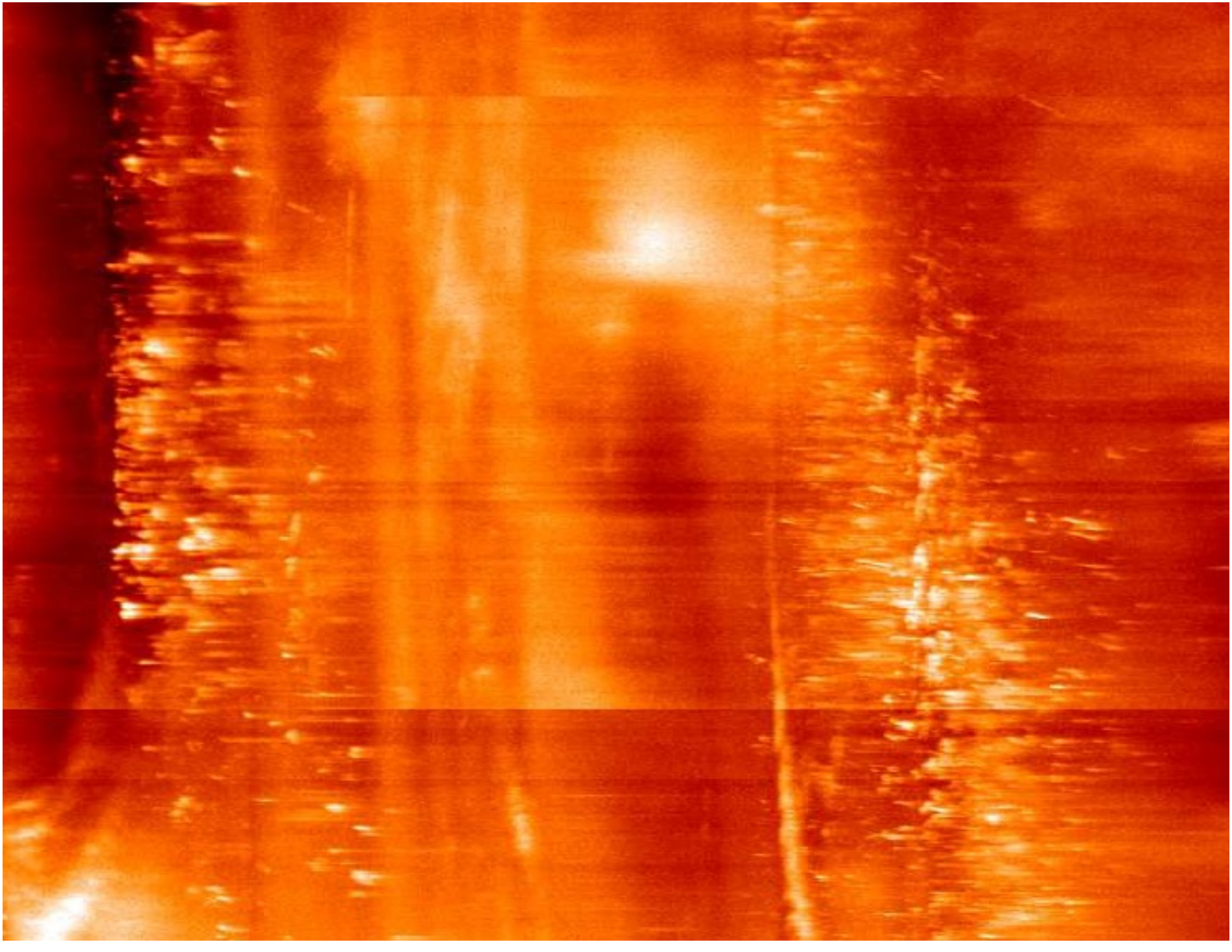

Structure in an (ordinary) solar noise storm

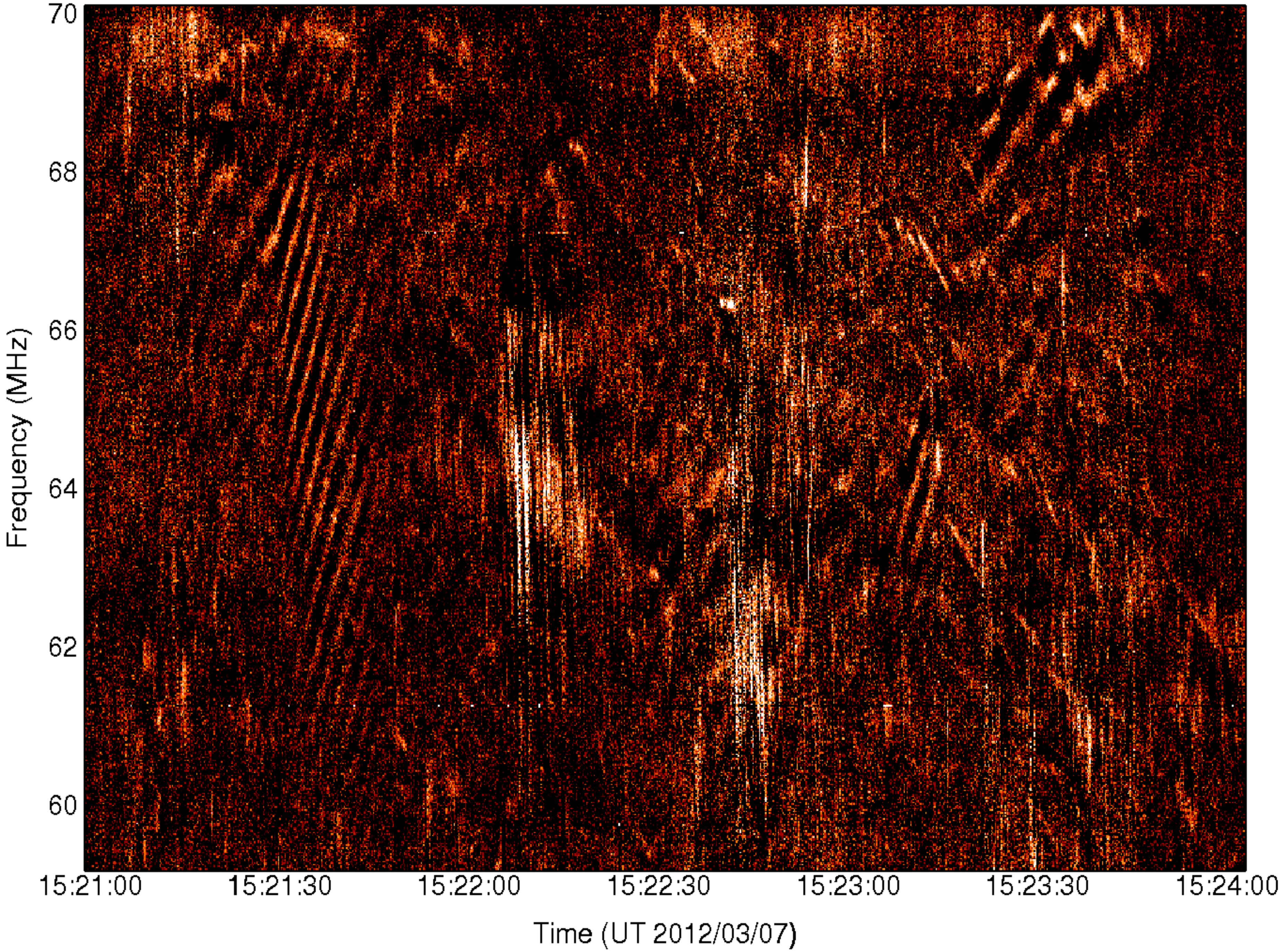

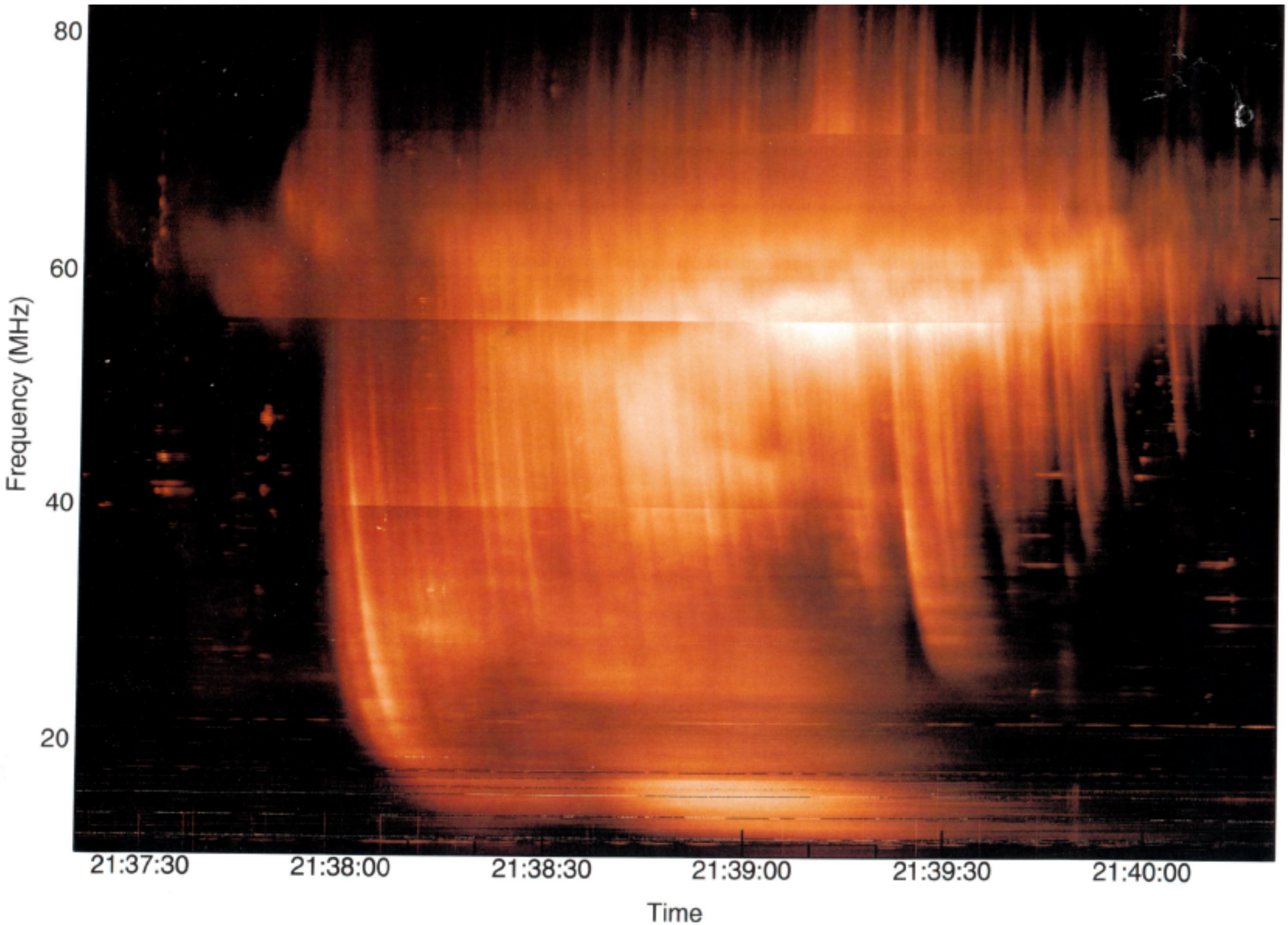

80
60
40
20
Frequency (MHz)
21:37:30
21:38:00
21:38:30
21:39:00
21:39:30
21:40:00
Time

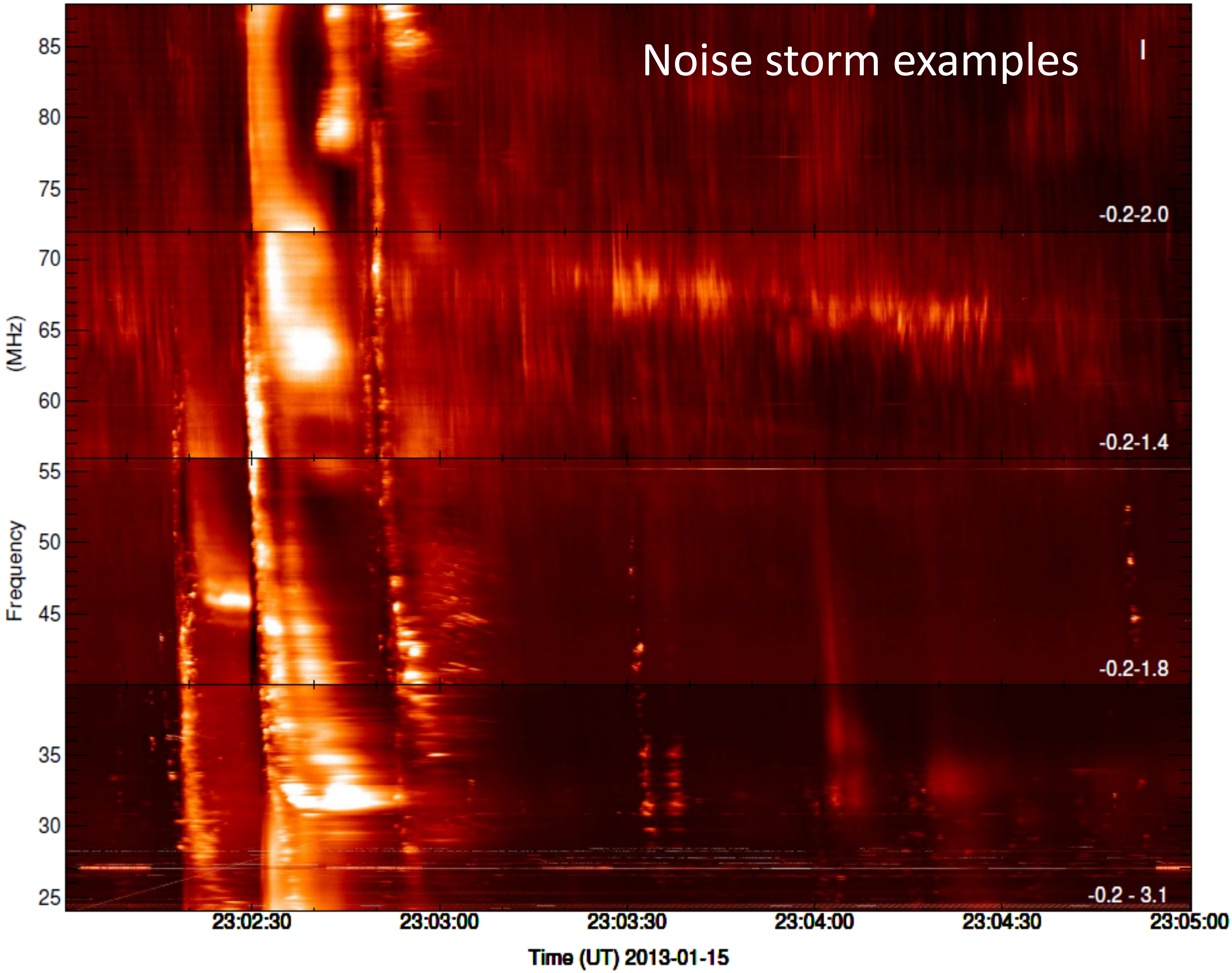

Noise storm examples
I
85
80
75
-0.2-2.0
70
65
60
-0.2-1.4
55
50
45
-0.2-1.8
35
30
25
-0.2 - 3.1
Frequency (MHz)
23:02:30
23:03:00
23:03:30
23:04:00
23:04:30
23:05:00
Time (UT) 2013-01-15

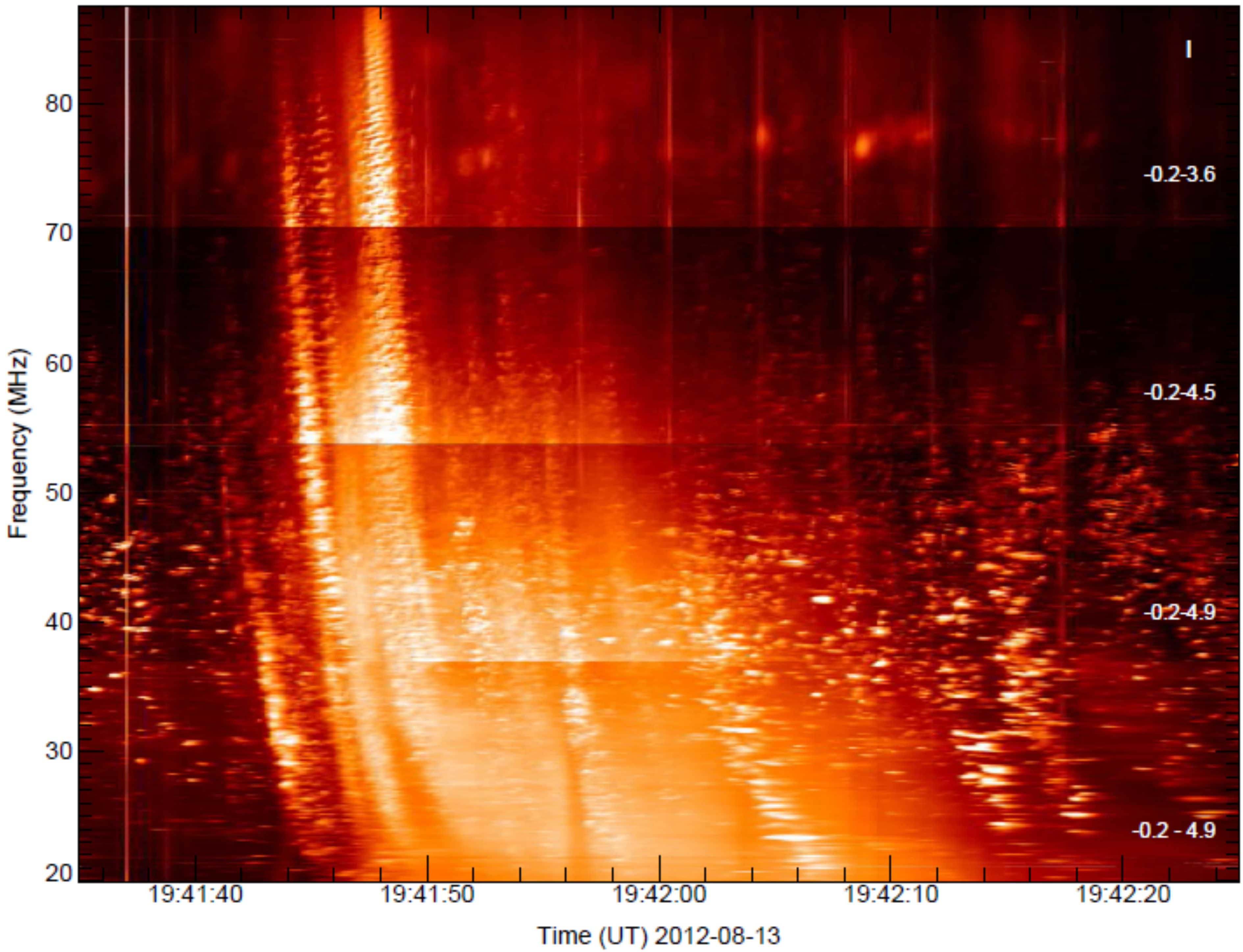

I
-0.2-3.6
-0.2-4.5
-0.2-4.9
-0.2 - 4.9
80
70
60
50
40
30
20
Frequency (MHz)
19:41:40
19:41:50
19:42:00
19:42:10
19:42:20
Time (UT) 2012-08-13

Fundamental and harmonic plasma emission

- Energetic electrons with free energy generate electrostatic Langmuir waves at frequency $f=f_p$, wavevector $\mathbf{k}=\mathbf{k}_p$.
- Since $k_p \gg f_p/c$, to produce propagating electromagnetic wave need to get rid of k
- To get fundamental emission, coalesce with low-frequency electrostatic wave such as ion sound with $\mathbf{k}_s \approx -\mathbf{k}_p$, $f_s \ll f_p$:

  $f_p + f_s = f_F \approx f_p$, $\mathbf{k}_p + \mathbf{k}_s = \mathbf{k}_F$, $k_F = f_F/c$
- A density depletion can "look like" a low frequency wave
- Scatter of electrostatic plasma waves off density inhomogeneity generates plasma waves with **k** opposite to original waves/beam
- Coalescence of two oppositely-directed plasma waves gives harmonic emission:

  $f_p + f_p = f_H \approx 2f_p$, $\mathbf{k}_p + (-\mathbf{k}_p) = \mathbf{k}_H$, $k_H = f_H/c$

Mechanisms of plasma emission

50 years of research on this topic. Two levels to the problem:
(i) beam propagation and interaction of beam and Langmuir waves;
(ii) generation of propagating electromagnetic emission.
Possible mechanisms include:

- Modulational instability: collapse of Langmuir wave packets. Requires very strong electric fields.
- Electrostatic decay: decay of Langmuir waves into low-frequency electrostatic waves and other Langmuir waves (L -> L' + S) or transverse waves (L -> T + S).
- Stochastic growth theory: time-integrated growth of Langmuir waves is a stochastic variable due to interactions between beam, waves and an inhomogeneous plasma that result in marginal stability. Predicts that waves should be bursty and irregular.

Fundamental and harmonic emission from a Type III burst

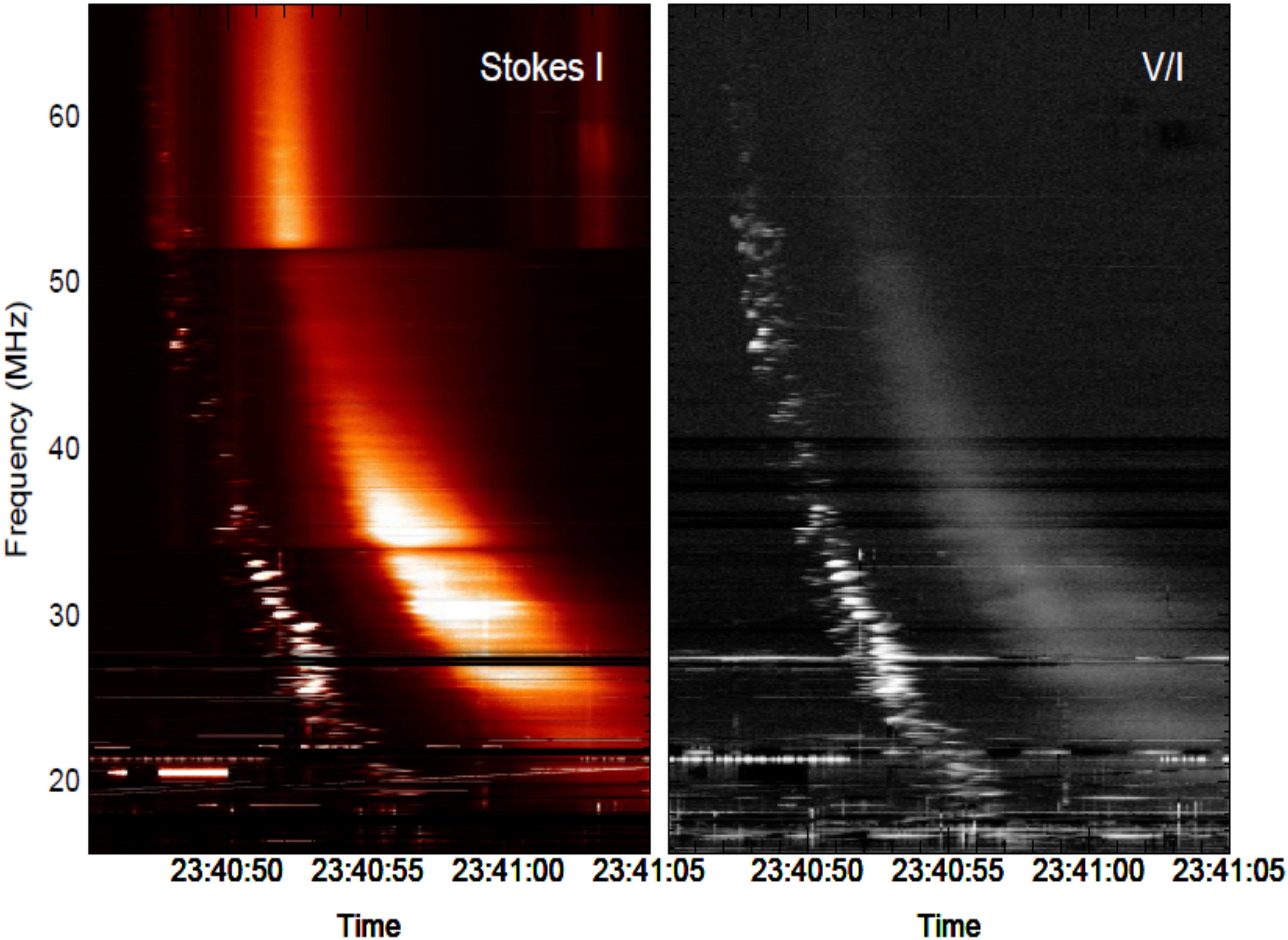

Striae details: narrowband, small if any drift

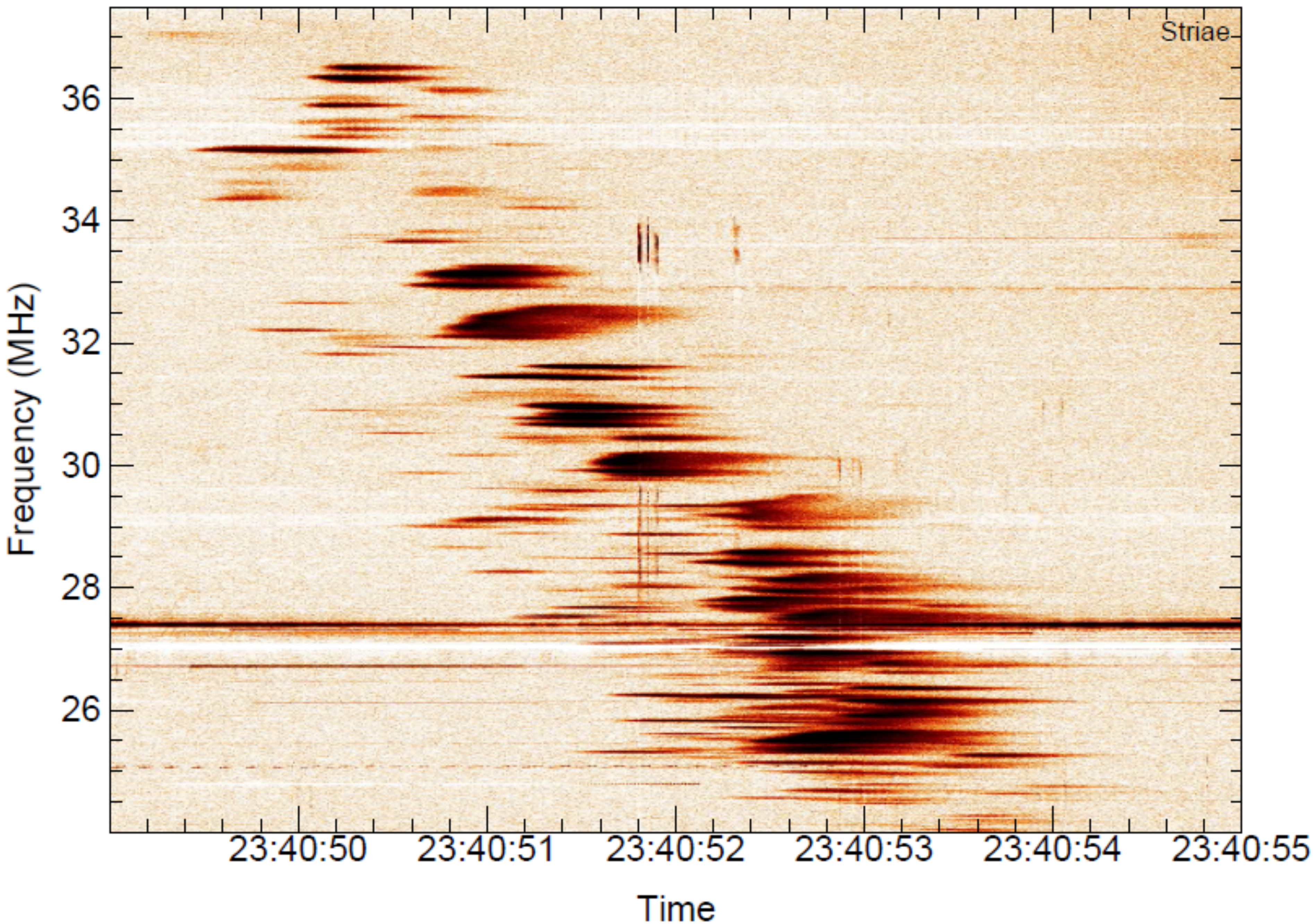

Fine structure in Type III bursts

- "Smooth" Type III bursts may be harmonic emission ($f = 2f_p$) while striae are fundamental emission ($f = f_p$): originally suggested because striae are more highly polarized.
- Models say that we can produce striae by local density enhancements (Takakura + Youssef 1975) in which the density gradient is small, source can be large, or
- by electron temperature enhancements, but only in the harmonic (Li et al 2011a), or
- by ion temperature enhancements, which make them more pronounced in the fundamental but emission is still weaker than $2f_p$ (Li et al 2011b).

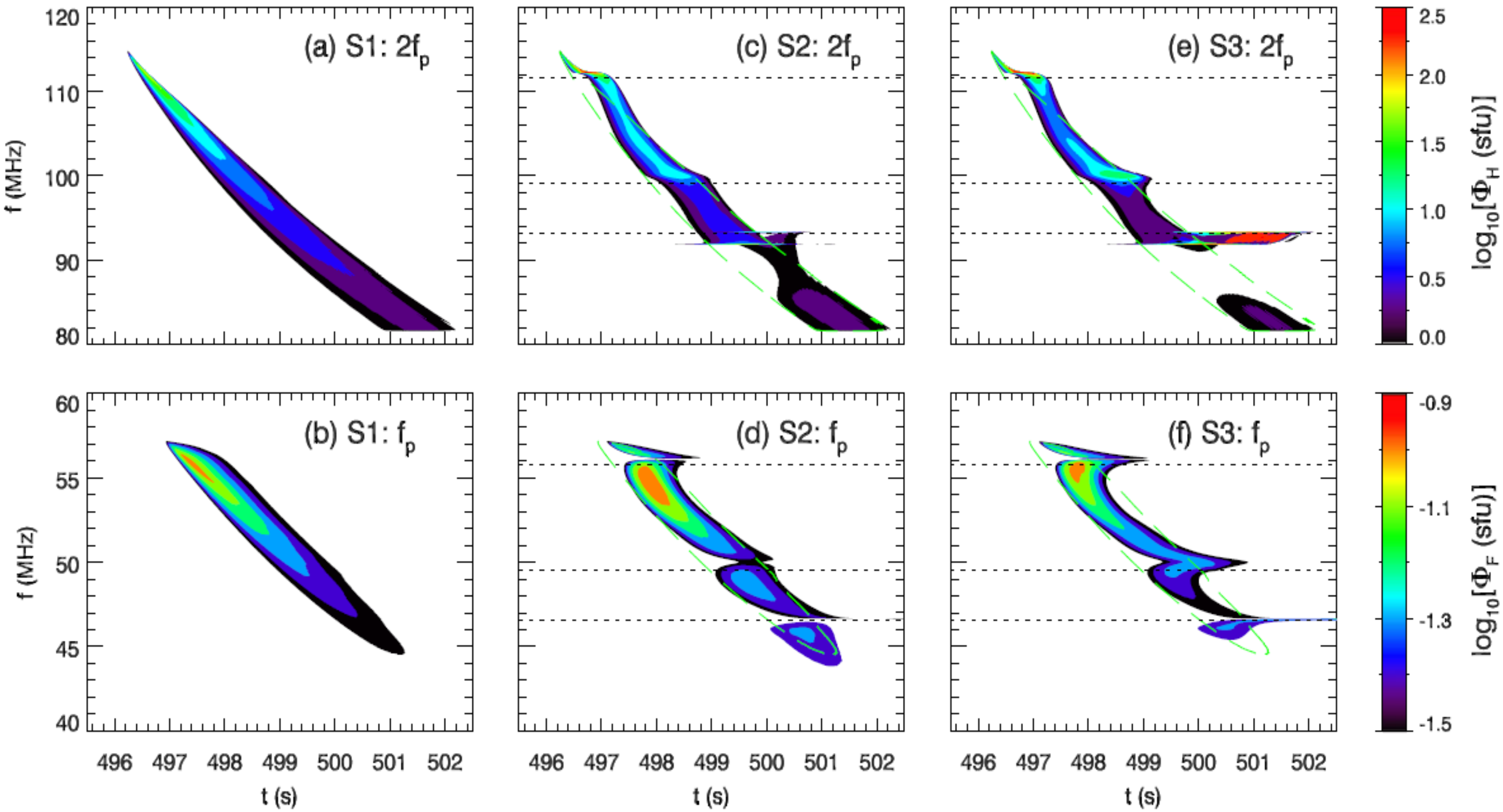

Smooth outward density gradient, fixed temperatures.

3 density fluctuations added to gradient, fixed temperatures.

3 density+T_e fluctuations, fixed T_i.

Simulations by Li et al 2012.

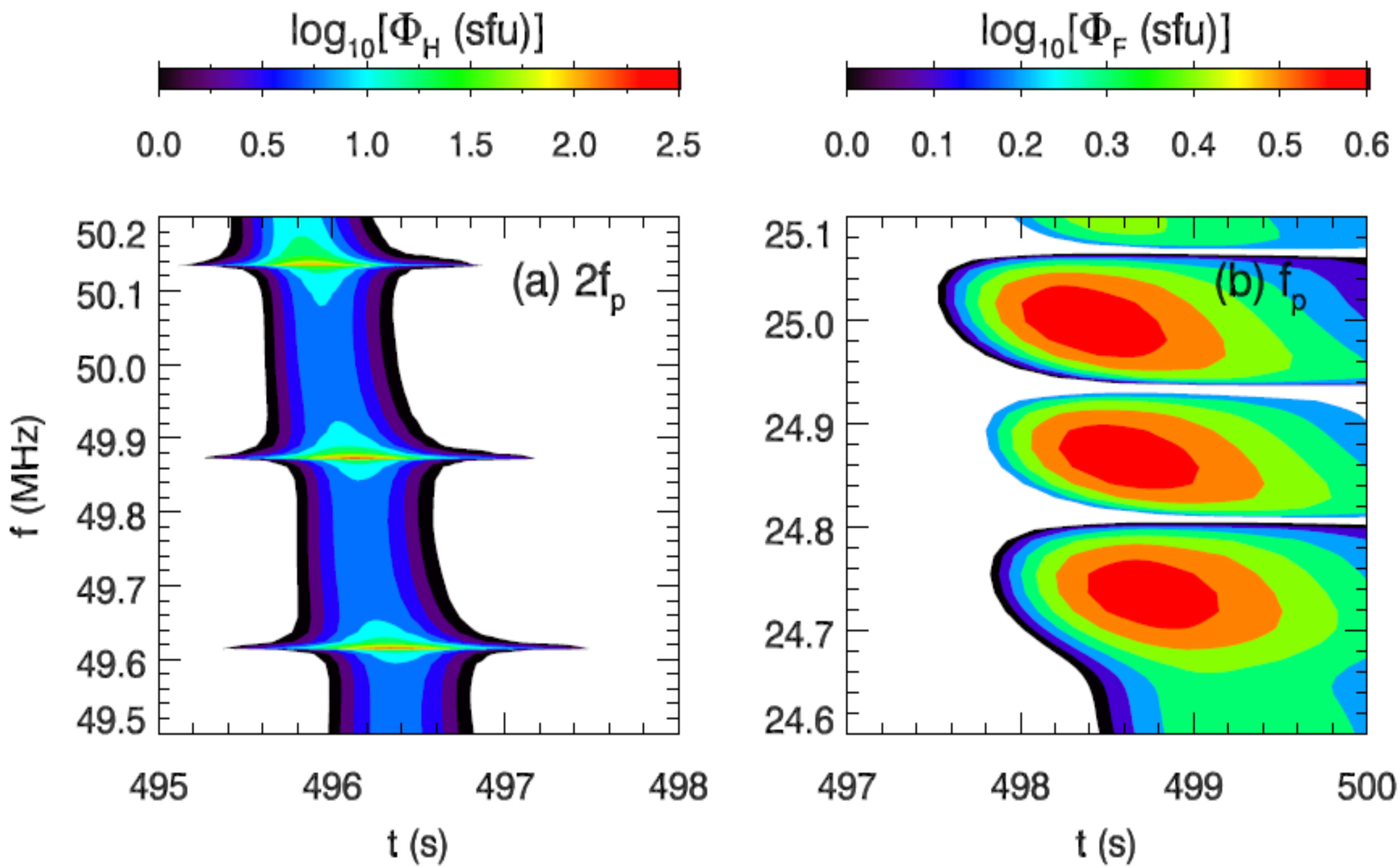

3 closely spaced density fluctuations added to gradient, fixed temperatures.

Simulations by Li et al 2012.

Structure in fundamental overlaid on harmonic

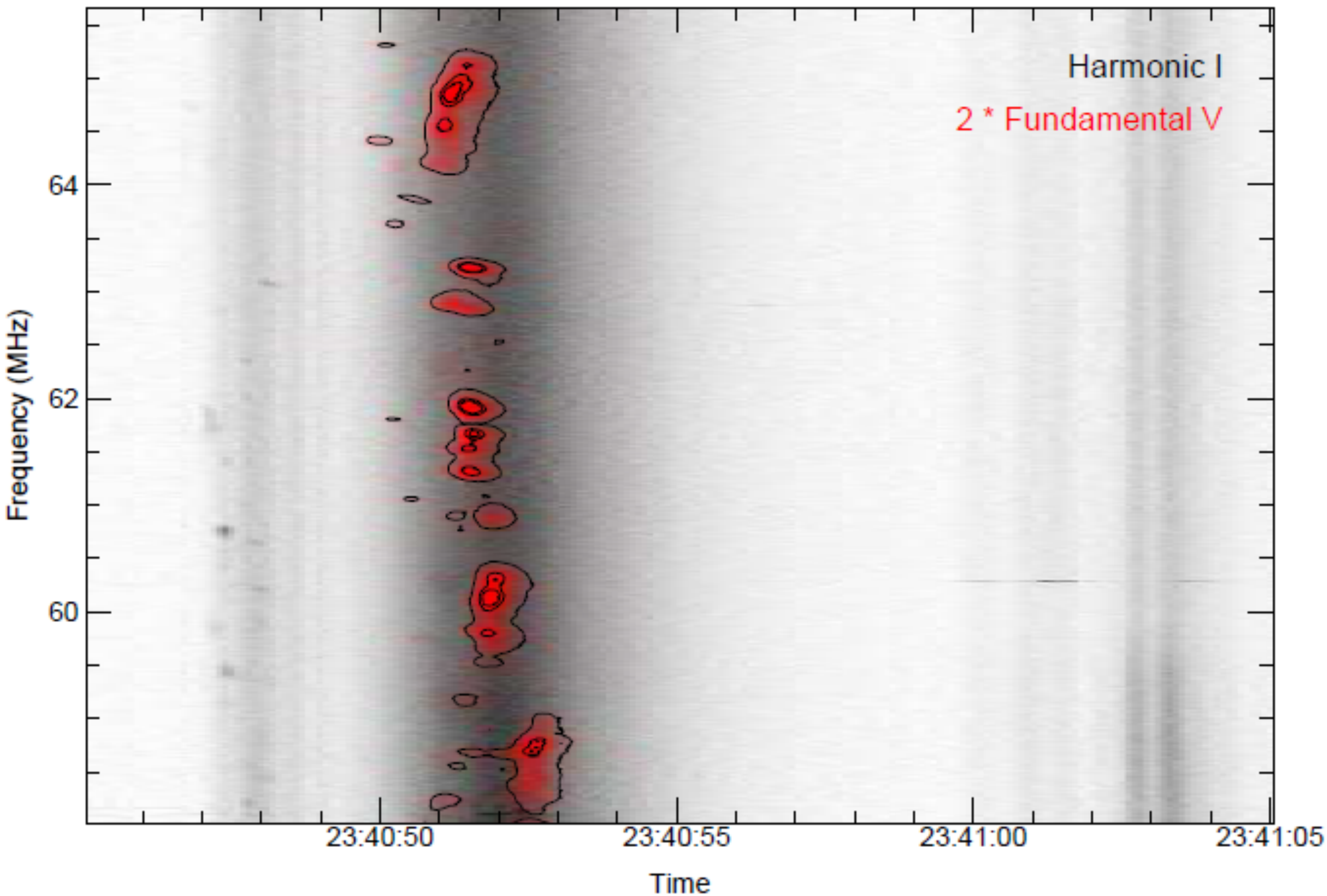

Structure in fundamental overlaid on harmonic

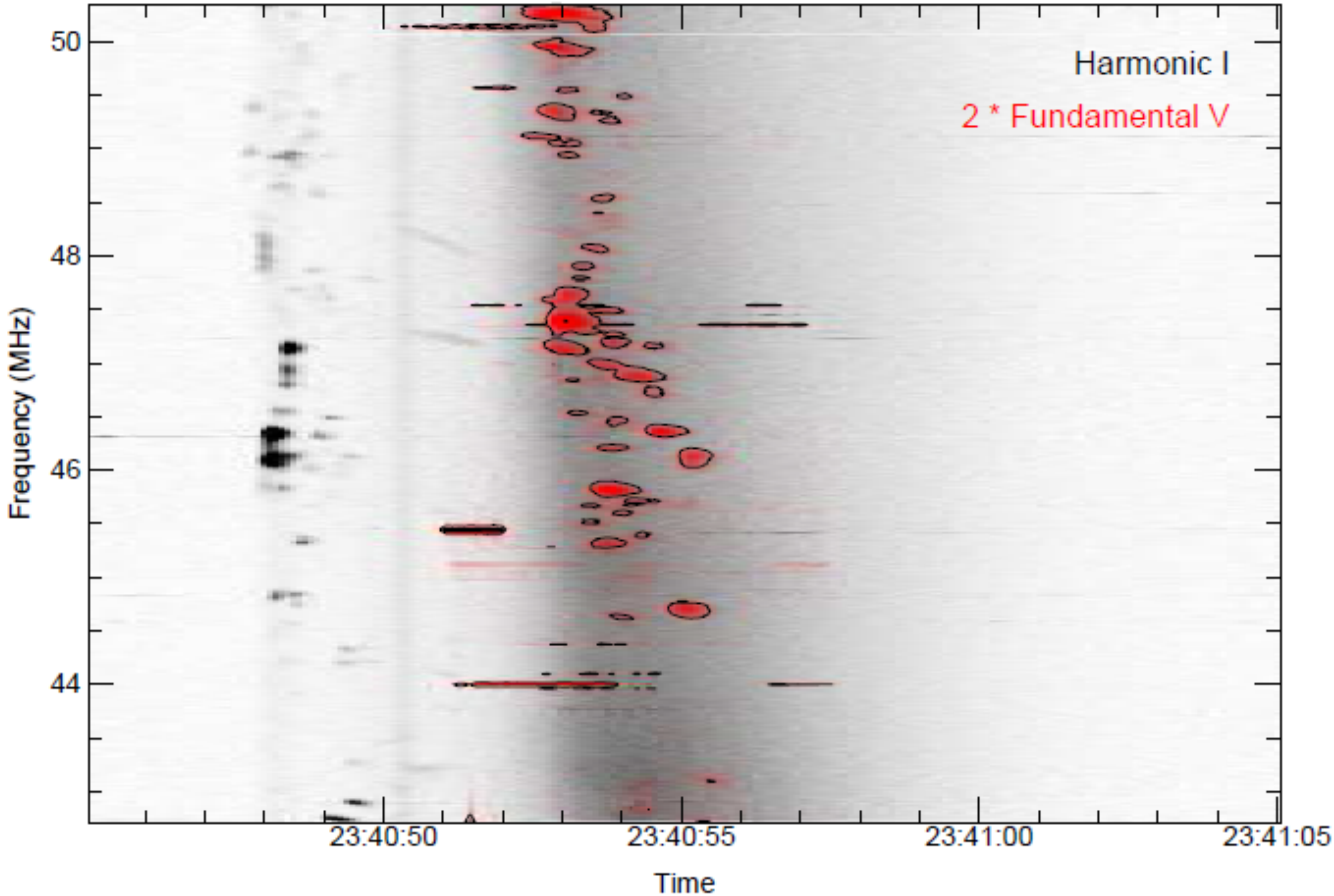

Striae at high resolution (10 millisec, 4 kHz)

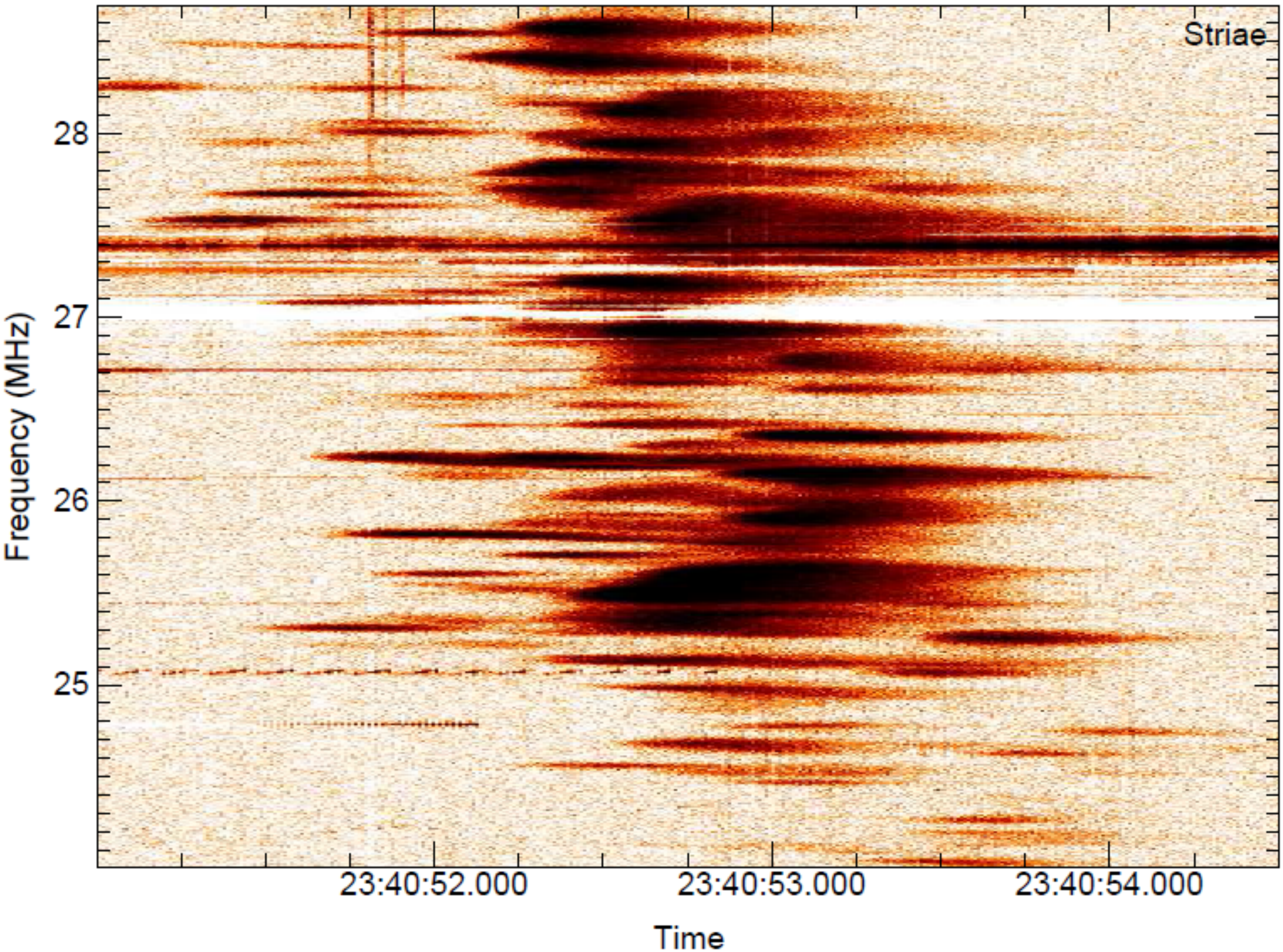

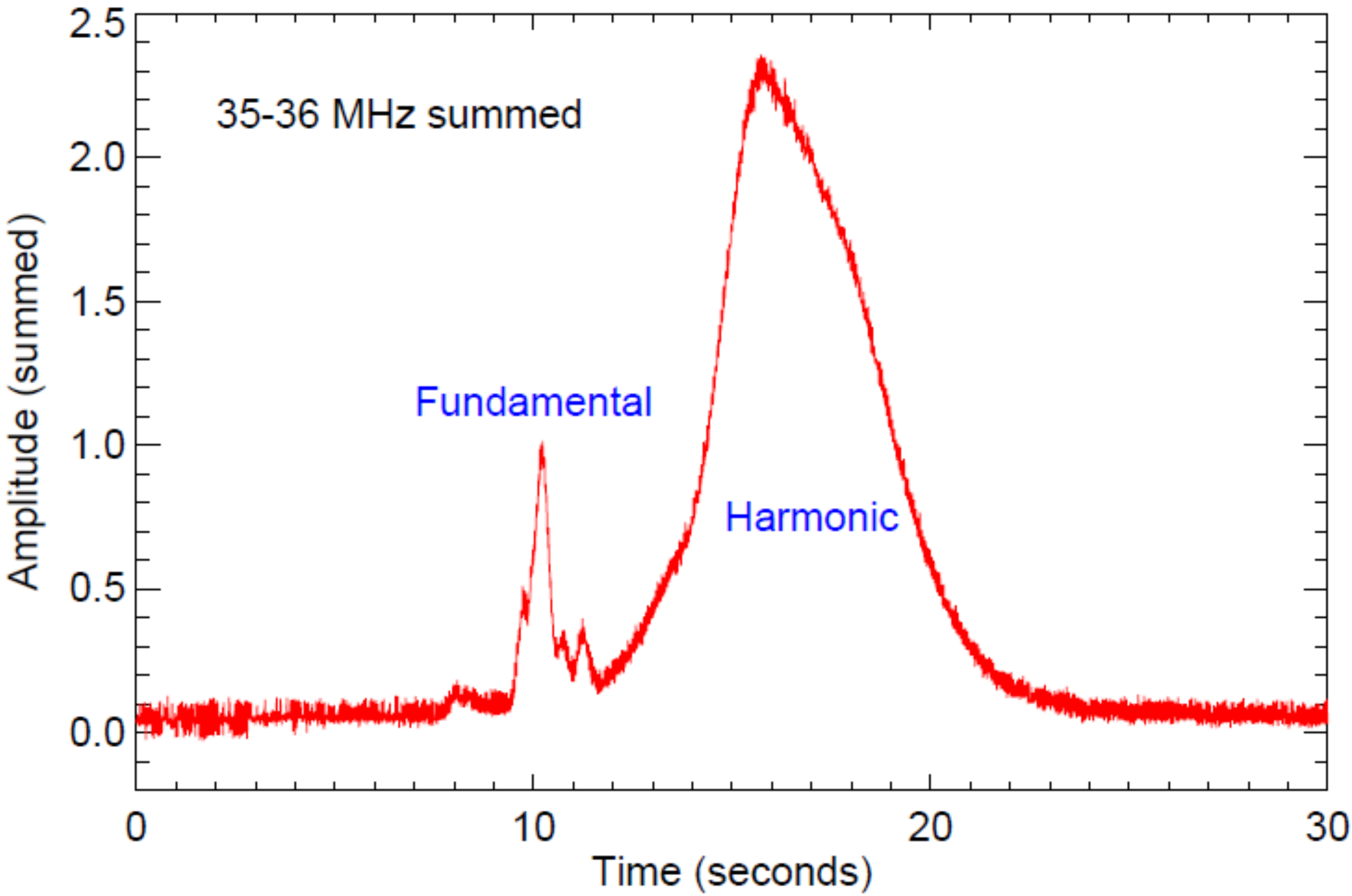

Harmonic profile is very smooth: Langmuir waves are smooth

Conclusions

- Models don't match what we see in the data: no striae in harmonic, fundamental brighter than harmonic
- No structure in harmonic, looks completely smooth
- Bright fundamental features start after corresponding harmonic emission: emission at fundamental does not care about Langmuir waves
- Bright fundamental structure depends on something else – density features? Localized low-frequency waves? Ducts?

An Imaging Example

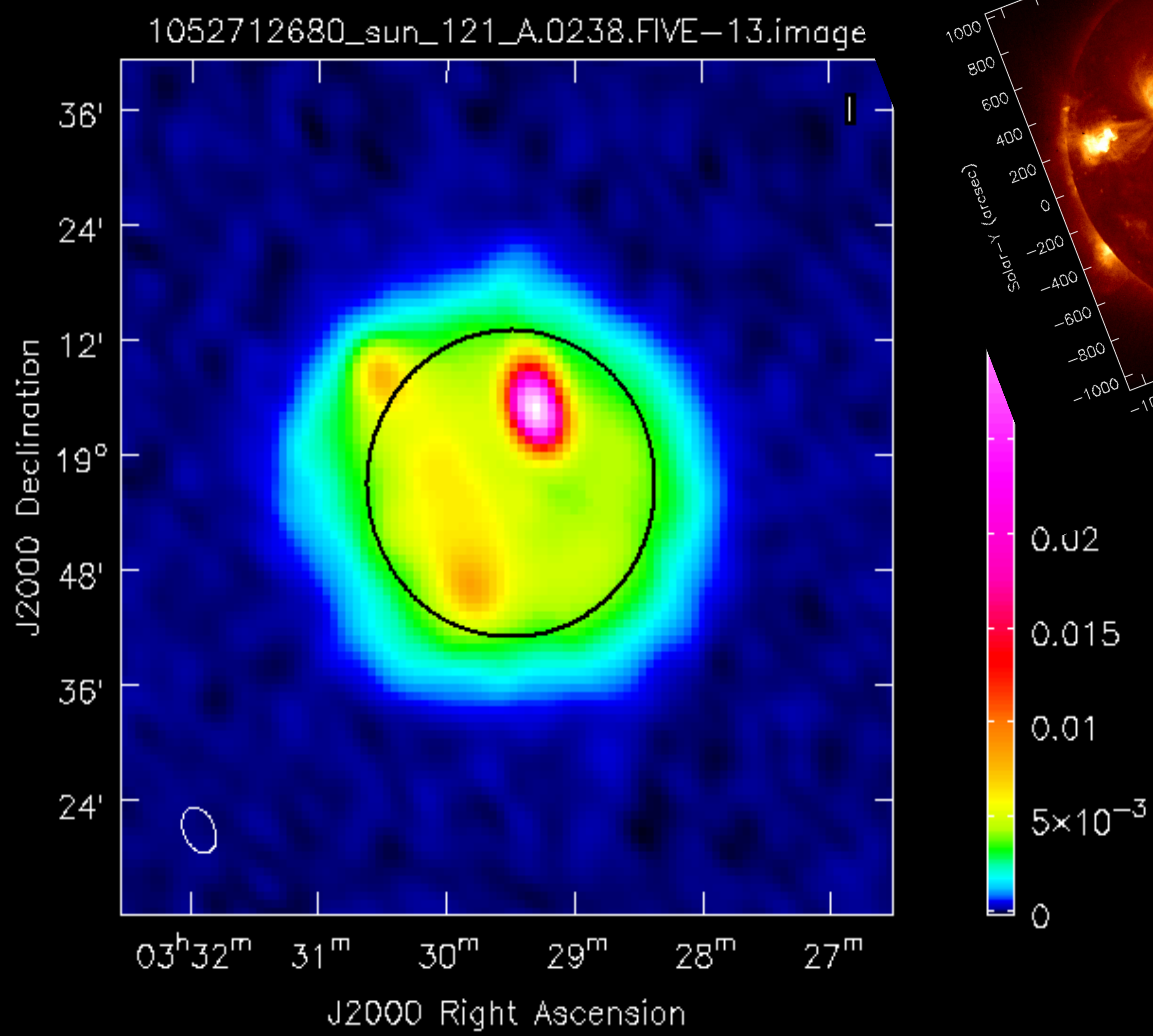

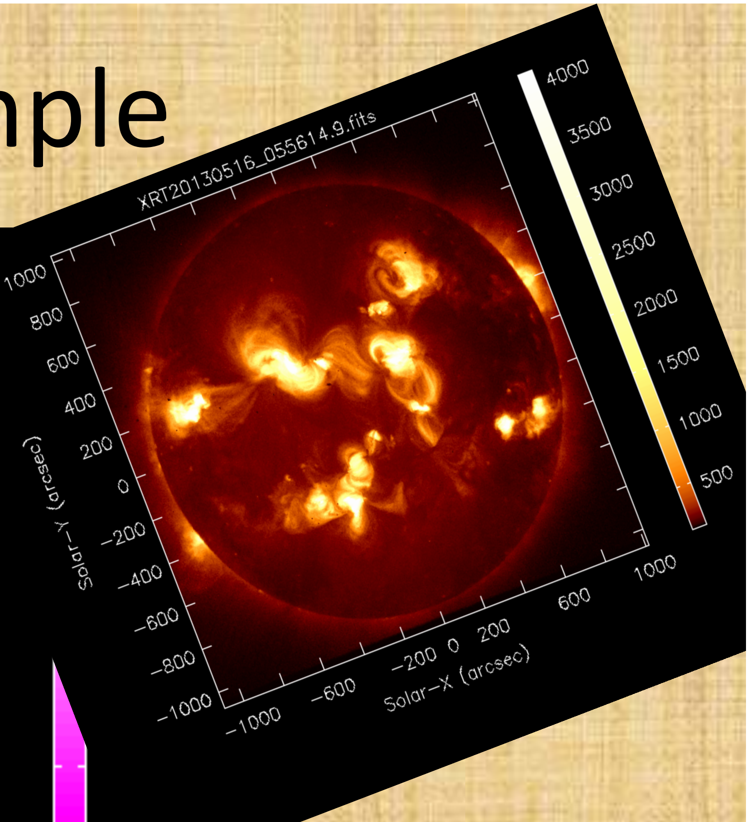

16 May, 2013
04:15:02 UT

ν_0=153.9 MHz
$\Delta\nu$=640 kHz
Δt=1 second
Dynamic
Range ~1400

Sample MWA Dynamic Spectrum

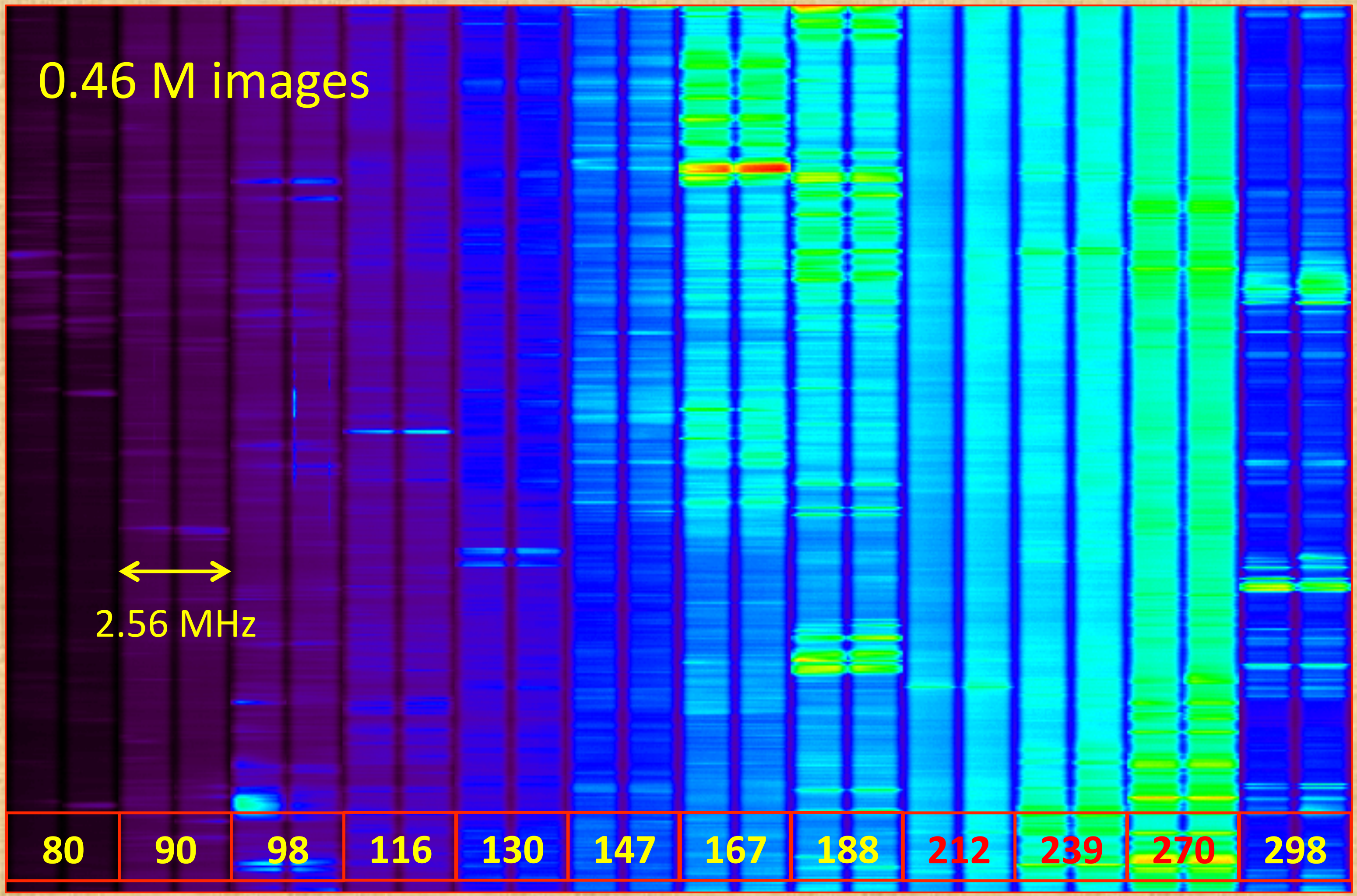

Time (5 min)

Frequency

(12 log-spaced groups of 2.56 MHz spanning 80 – 300 MHz)